Washington University in St. Louis
Washington University Open Scholarship

Engineering and Applied Science Theses & Dissertations | McKelvey School of Engineering

Spring 5-2014

Numerical Simulation and Optimization of Carbon Dioxide Utilization and Storage in Enhanced Gas Recovery and Enhanced Geothermal Systems

James H. Biagi
Washington University in St Louis

Follow this and additional works at: https://openscholarship.wustl.edu/eng_etds

 Part of the Mechanical Engineering Commons

Recommended Citation

Biagi, James H., "Numerical Simulation and Optimization of Carbon Dioxide Utilization and Storage in Enhanced Gas Recovery and Enhanced Geothermal Systems" (2014). *Engineering and Applied Science Theses & Dissertations*. 6.
https://openscholarship.wustl.edu/eng_etds/6

This Thesis is brought to you for free and open access by the McKelvey School of Engineering at Washington University Open Scholarship. It has been accepted for inclusion in Engineering and Applied Science Theses & Dissertations by an authorized administrator of Washington University Open Scholarship. For more information, please contact digital@wumail.wustl.edu.

WASHINGTON UNIVERSITY IN ST. LOUIS
School of Engineering and Applied Science
Department of Mechanical Engineering and Materials Science

Thesis Examination Committee

Dr. Ramesh K. Agarwal (Chair)

Dr. David A. Peters

Dr. Kenneth Jerina

Numerical Simulation and Optimization of Carbon Dioxide Utilization and Storage in Enhanced Gas Recovery and Enhanced Geothermal Systems

by

James H. Biagi

A thesis presented to the School of Engineering and Applied Science
of Washington University in partial fulfillment of the
requirements for the degree of
Master of Science

May 2014

Saint Louis, Missouri

Table of Contents

List of Figures

List of Tables

List of Abbreviations

CCS – Carbon Capture and Sequestration

CCUS – Carbon Capture Utilization and Sequestration

EGR – Enhanced Gas Recovery

CSEGR – Carbon Storage and Enhanced Gas Recovery

EOR – Enhanced Oil Recovery

EGS – Engineered Geothermal System

CFD – Computational Fluid Dynamics

IFD – Integral Finite Difference

TOUGH2- **T**ransport **O**f **U**nsaturated **G**roundwater and **H**eat (Version 2)

Acknowledgments

I would like to thank Professor Ramesh K. Agarwal for his consistent support throughout my research, his patience through my struggles, and his devotion as a leader in my research. I would also like to thank Zheming Zhang for sharing his wide breadth of knowledge and experience of subsurface flow modeling. Earlier work on the GA optimization module done by Morgan Brandon and Zheming Zhang has been very helpful.

I would like to thank my parents for their constant development of my curiosity and their support of my educational pursuits.

James H. Biagi

Washington University in St. Louis
May 2014

ABSTRACT OF THE THESIS

Numerical Simulation and Optimization of Carbon Dioxide Utilization and Storage in Enhanced Gas Recovery and Enhanced Geothermal Systems

by

James H. Biagi

Department of Mechanical Engineering and Materials Science

Washington University in St. Louis, 2014

Research Advisor: Professor Ramesh K. Agarwal

Abstract

With rising concerns surrounding CO_2 emissions from fossil fuel power plants, there has been a strong emphasis on the development of safe and economical Carbon Capture Utilization and Storage (CCUS) technology. Two methods that show the most promise are Enhanced Gas Recovery (EGR) and Enhanced Geothermal Systems (EGS). In Enhanced Gas Recovery a depleted or depleting natural gas reservoir is re-energized with high pressure CO_2 to increase the recovery factor of the gas. As an additional benefit following the extraction of natural gas, the reservoir would serve as a long-term storage vessel for the captured carbon. CO_2 based Enhanced Geothermal Systems seek to increase the heat extracted from a given geothermal reservoir by using CO_2 as a working fluid. Carbon sequestration is accomplished as a result of fluid losses throughout the life of the geothermal system. Although these technologies are encouraging approaches to help in the mitigation of anthropogenic CO_2 emissions, the detailed mechanisms involved are not fully understood. There remain uncertainties in the efficiency of the systems over time, and the safety of the sequestered CO_2 due to leakage. In addition, the efficiency of both natural gas extraction in

EGR and heat extraction in EGS are highly dependent on the injection rate and injection pressure. Before large scale deployment of these technologies, it is important to maximize the extraction efficiency and sequestration capacity by optimizing the injection parameters.

In this thesis, numerical simulations of subsurface flow in EGR and EGS are conducted using the DOE multiphase flow solver TOUGH2 (Transport of Unsaturated Groundwater and Heat). A previously developed multi-objective optimization code based on a genetic algorithm is modified for applications to EGR and EGS. For EGR study, a model problem based on a benchmark-study that compares various mathematical and numerical models for CO_2 storage is considered. For EGS study a model problem based on previous studies (with parameters corresponding to the European EGS site at Soultz) is considered. The simulation results compare well with the computations of other investigators and give insight into the parameters that can influence the simulation accuracy. Optimizations for EGR and EGS problems are carried out with a genetic algorithm (GA) based optimizer combined with TOUGH2, designated as GA-TOUGH2. Validation of the optimizer was achieved by comparison of GA based optimization studies with the brute-force run of large number of simulations. Using GA-TOUGH2, optimal time-independent and time-dependent injection profiles were determined for both EGR and EGS. Optimization of EGR problem resulted in a larger natural gas production rate, a shorter total operation time, and an injection pressure well below the fracture pressure. Optimization of EGS problem resulted in a precise management of the production temperature profile, heat extraction for the entire well life, and more efficient utilization of CO_2. The results of these studies will hopefully pave the way for future GA-TOUGH2 based optimization studies to improve the modeling of CCUS projects.

Chapter 1

Introduction

1.1 Energy Consumption and its Effects on Environment

With the rise of the industrial revolution at the turn of the 20th century, the world began to consume fossil fuel energy at an astonishing rate. Some of the uses of this energy include power generation, transportation, heating and cooling of buildings, industrial production, water supply, and waste processing. The availability of these services and products have become part of everyday life are essential to our everyday life, and have enabled the human civilization to technologically advance at an ever-increasing pace with greater standard of living and quality of life. Current estimates of energy usage approach 500 quadrillion Btu with projections of near 800 quadrillion Btu by 2040. Although renewable energy is predicted to account for an increasing amount of the energy supply in the future, fossil fuels will remain the dominant energy source for the next 25 years [1].

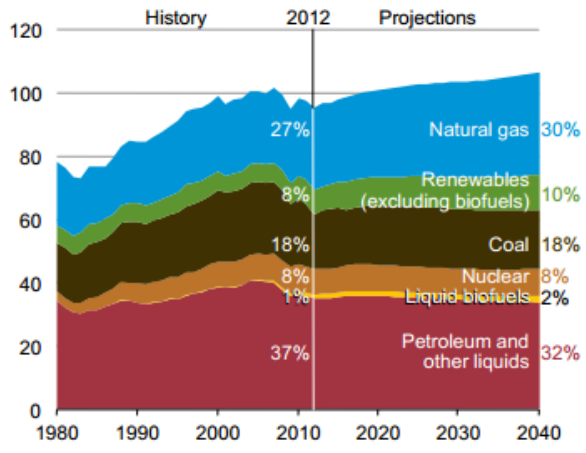

Figure 1.1: Historical world energy consumption and projections [1]

In many ways fossil fuels are an ideal energy source, they are relatively easy to access, efficient, affordable, and their characteristics are widely known. However, it is well established by the scientific community that the use of fossil fuels is resulting in pollution of air and water, including greenhouse gas (GHG) emissions. There is substantial support that the burning of fossil fuels adversely affects the environment and may lead to global warming causing disastrous consequences to the ecosystems and inhabitants of the earth. One of the chief causes is the increasing concentrations of the greenhouse gas carbon dioxide (CO_2) in the atmosphere due to anthropogenic emissions. The combustion of fossil fuels (oil, coal, natural gas) releases CO_2 into the atmosphere as a by-product. While its concentrations may seem relatively small in the short term period of a few years, CO_2 takes a substantial amount of time to decay and can remain in the atmosphere for hundreds of years. This can lead to an increase in atmospheric concentration of CO_2 as the current rate of its release in the atmosphere can compound on the emissions of the past. Since 1960, atmospheric CO_2 levels have risen dramatically from near 315 ppm to current levels approaching 400 ppm [2]. CO_2 emissions have been steadily rising since the beginning of the 20th century, during the early 1900's total emissions hovered around 2,500 teragrams of CO_2, they have steadily risen to present levels greater than 30,000 teragrams [3].

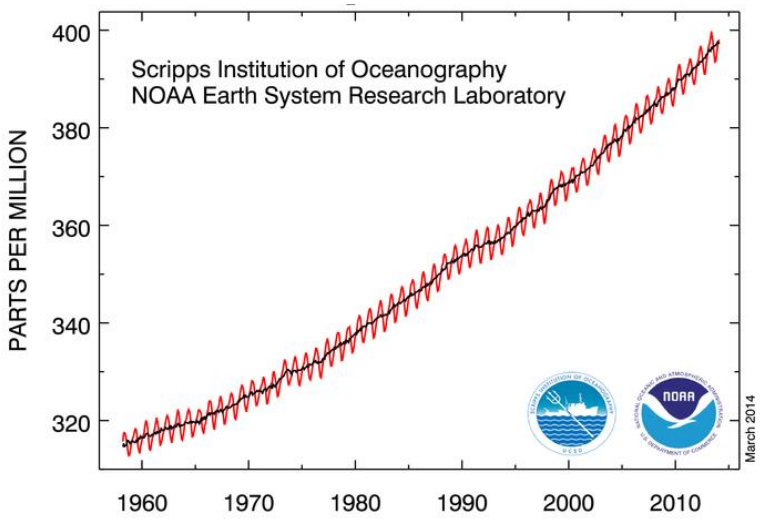

Figure 1.2: Atmospheric concentrations of CO_2 recorded at Mauna Loa Observatory [2]

Numerous recent studies have suggested a strong correlation between the increased concentration of anthropogenic CO_2 and the increase in the Earth's average surface temperature. Global warming can lead to dramatic changes in short-term weather as well as long term effects on climate and ecosystems. Global warming may result in rising sea levels, ocean acidification, changes in precipitation patterns, and the expansion of subtropical deserts. Additional effects may include increases in extreme weather events, species displacement and extinction, and diminished agricultural yields. Left unchecked, global warming has the potential to cause catastrophic effects to the Earth's ecosystems and human society. There is a significant need to develop technologies to mitigate the effects of CO_2 on our atmosphere.

1.2 Geological Carbon Sequestration/Utilization

Carbon capture and geological sequestration (CCGS) offers a potential solution to reduce a large amount of direct CO_2 emissions. The long-term geological storage of CO_2 can help stabilize the CO_2 concentration in the atmosphere and therefore reduce the CO_2 concentrations in the atmosphere. In

a typical CCGS project, carbon is captured at significant emitters of CO_2 such as power plants, and then permanently stored (sequestered) in a nearby underground geologic formation. Geological formations such as saline aquifers, oil fields, un-mineable coal seams, basalt-formations, or gas fields are chosen as potential sequestration sites. These formations have a highly permeable reservoir capped with a nearly impermeable layer of rock. The cap-rock prevents the leakage of CO_2 from the natural reservoir. When implemented to its full capacity, it is estimated that the CCGS process may reduce CO_2 emissions from power plants and other stationary sources by 80~90 percent compared to the same operation without CCGS [3].

1.2.1 Trapping Mechanisms in Geological Carbon Storage

Under the Earth's crust there are many layers of geological formations with differing hydrogeological and thermodynamic properties. A reservoir forms when one geologic formation with a high porosity is overlain by a formation of low porosity. The high porosity region allows subsurface fluid such as oil, gas, or saline to be contained in a relatively higher ratio than would be present in lower porosity structures. The surrounding of the reservoir by a low porosity and low permeability layer results in the containment of the fluid to the reservoir itself. These reservoirs are present all over the world and some may serve as prime candidates for long term CO_2 storage. The CCGS process begins with the capture of CO_2 from large, stationary emitters such as a coal power plant or large industrial facility. The CO_2 is then compressed and transported to the injection site where it is injected into a predetermined geologic formation for permanent storage.

Once present in the geologic formation the CO_2 undergoes four distinct trapping mechanisms to ensure its complete and permanent storage in the reservoir. These mechanisms are described further below, Figure 1.3 shows the time-scales, storage contributions, and security of the mechanisms [4].

1. Structural and stratigraphic trapping: This mechanism employs the physical properties of the reservoir and the injected CO_2 to ensure a complete trapping. The formation is surrounded by an upper, lower, and lateral confining formation to eliminate any CO_2 migration out of the reservoir. Of these formations the upper formation or cap-rock is particularly important to limit the buoyant migration of the injected CO_2. Structural and stratigraphic trapping is the first stage in GCS and is responsible for trapping the majority of the CO_2 during its initial injection. It is however the least secure mechanism as it has a high risk of leakage.
2. Residual trapping: The voids of the storage formation originally held fluid such as saline, natural gas, or oil. With the injection of CO_2 some of the in situ fluid will be driven out of the system and be replaced with CO_2. As the CO_2 moves through the reservoir some parts become separated from the plume or are left behind as disconnected droplets in pore space. These isolated droplets remain immobile due to the capillary pressure surrounding them. This process is referred to as residual trapping; it has a relatively small capacity but is more secure than structural and stratigraphic trapping.
3. Solubility trapping: Once present in the reservoir, the injected CO_2 begins to mix and dissolve into the original formation fluid. The formation fluid with the CO_2 becomes slightly denser than the surrounding fluid and thus sinks to the bottom of the formation where it is trapped. Although this process is a more secure storage method than the previous two mentioned, it is a very long process and its success depends on the in situ reservoir fluid. For example, brine water may serve as a better conduit for solubility trapping than natural gas as CO_2 may dissolve more easily into brine.
4. Mineral trapping: The dissolved CO_2 into the reservoir fluid will often result in a weak carbonic acid. Over very large time scales, this carbonic acid is predicted to interact with the rocks and minerals in the formation to form new carbonate minerals as precipitates. The

formation of these carbonate minerals is the last stage in CO_2 storage and is considered to be the most permanent mechanism.

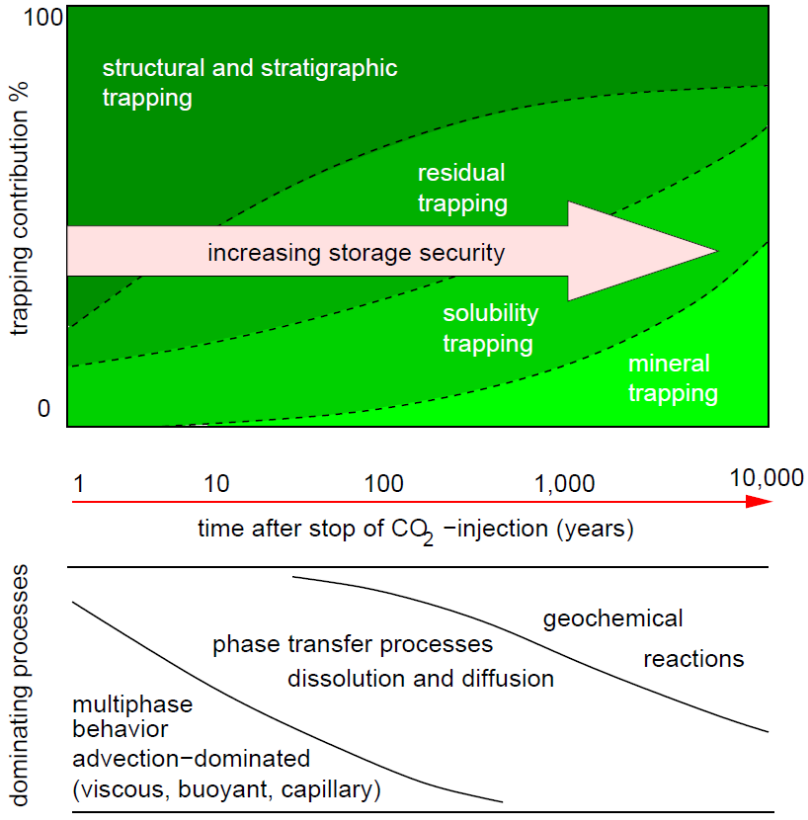

Figure 1.3: Trapping mechanisms, their timeframes, storage contribution and security [5]

1.2.2 Carbon Capture Utilization and Storage (CCUS)

Carbon Capture Utilization and Storage is the process of using captured CO_2 for enhanced oil recovery (EOR), enhanced gas recovery (EGR), or enhanced geothermal systems (EGS). While CCS projects seek to simply store captured carbon, the goal of CCUS projects is to use the CO_2 to benefit

further energy production. Figure 1.4 shows a schematic of potential CCUS projects. The power plant employs carbon capture technology to separate a nearly pure CO_2 stream from its exhaust. The captured CO_2 is then injected deep underground into a geological formation where it can be utilized for EOR, EGR, or EGS.

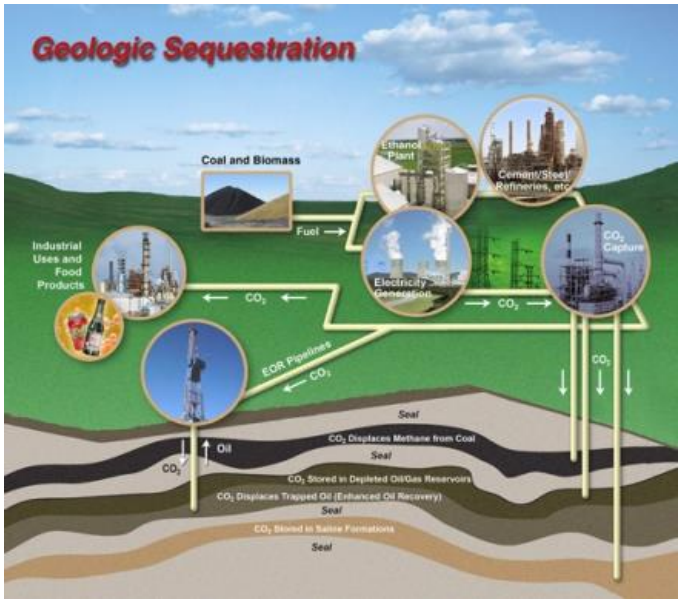

Figure 1.4: A schematic of potential CCUS projects [6]

Enhanced Oil Recovery employs highly pressurized CO_2 in order to increase the recovery factor of an oil well. In deep oil reservoirs where CO_2 becomes supercritical, CO_2 is miscible with oil. This results in reduction in the oil viscosity, a reduction in its surface tension with the surrounding rock, and a swelling effect, all of which make the oil more mobile in the reservoir. Enhanced Oil Recovery is regularly used in the US and other countries of the world. The US Department of Energy (DOE) estimates that there are over 100 commercial CO_2 injection projects used for EOR. Most of the CO_2 used in EOR is piped from surrounding natural CO_2 sources, however recent advancements in technology may allow for captured CO_2 from large stationary sources to be used economically [6]. The DOE has estimated that further development of CCS integrated EOR in the United States will

be necessary to generate substantial additional oil resources [6]. The process of EOR is well documented, and has been in use for many decades. The results are promising and provide some insight into the possibility of sustained Carbon Capture and Utilization.

Following the Enhanced Oil Recovery methodology, it has been proposed that captured carbon dioxide could also be used for enhanced natural gas extraction with large recovery factor. In EGR, CO_2 is injected into a depleted natural gas reservoir to enhance CH_4 extraction by displacement and re-pressurization of the reservoir. This is an economically advantageous approach since the recovered CH_4 can be sold to offset the cost of CO_2 sequestration. In addition, the reservoir may be more capable of long-term storage of CO_2 since it already contains a fluid of lighter density. The concept of Carbon Sequestration with Enhanced Gas Recovery (CSEGR) was originally proposed by van der Burgt et al. (1992) and Blok et al., (1997)[7],[8]; however the idea did not receive much attention due to the historically high price of CO_2, and concerns about CO_2 contamination in the produced gas. With advancements in Carbon Capture technologies as well as possible government mandates to limit CO_2 emissions, CSEGR is likely to become more economically viable.

In addition to EOR and EGR, another method for utilization of captured CO_2 that is receiving much attention in recent years is referred to as the Enhanced Geothermal System (EGS). The idea, first brought forth by Donald Brown in 2000, suggests that CO_2 may have significant advantages over water as a working fluid for EGS. [9] The important advantages of employing CO_2 are:

1. It is a poor solvent for most rock minerals
2. It has a large compressibility and expansivity leading to a higher natural buoyancy force and a reduction in necessary pumping power
3. A lower comparative viscosity to water resulting in a higher mobility for certain thermodynamic conditions.

4. The potential to permanently sequester CO_2 through fluid losses during the operation of the system.

Because of these benefits of CO_2, Brown proposed using supercritical CO_2 as a working fluid in Enhanced Geothermal Systems. He proposed a preliminary study comparing a system operating with water to that operating with supercritical CO_2. Following up on Brown's original idea, researchers have been working diligently to investigate potential of Carbon Dioxide usage in an EGS.

Typically a specific area in the reservoir that has high permeability is targeted and then fractured to allow for higher flow rates. Most Enhanced Geothermal Systems are developed for a reservoir initially containing water and brine. CO_2 is then be pumped into the reservoir at an injection site, and as a result an aqueous mixture of water and salt would flow out of the production well. With increased CO_2 injection the flow stream will contain an increasing percentage of CO_2 in the outflow from the reservoir. Once the desired reservoir conditions are established and a constant stream of CO_2 flows in and out of the reservoir, the heat extraction from the reservoir fluid takes full effect. Once the heat is extracted from the fluid, the CO_2 is pumped back into the reservoir at a supercritical state. This cycle continues throughout the life cycle of the geothermal reservoir with a migrating cold front from the injection to production well. Sequestration of CO_2 occurs through subsurface fluid losses through the reservoir and its surrounding subsurface structures. Typical fluid losses for water-based systems approach 5%, and thus a similar loss may be approximated for CO_2. [10]. Contrary to that of water-based EGS, fluid losses in CO_2-based EGS are beneficial as it provides a permanent storage for the some of the injected CO_2.

1.3 Current GCS and CCUS Projects

During the 1990's the world's first commercial GCS project was commissioned at the Sleipner gas field in the North Sea off the coast of Norway. Since this initial project, a number of additional GCS and CCUS projects have been proposed and implemented. Some examples of the pilot and demonstration projects are listed below [11].

- Sleipner West (Norway): Statoil and the International Energy Agency began injecting supercritical phase CO_2 into the Utsira saline formation under the North Sea in 1996. The project is still in operation today and has served as a great resource for GCS and CCUS.
- Weybrun CO_2 Flood Project (Canada): EnCana and the IEA began storing and utilizing CO_2 in conjunction with enhanced oil recovery in 2000. During the initial phase, seven million tons of CO_2 was stored, subsequent phases have focused on leakage risks, monitoring CO_2 migration, and performance efficiency.
- Shute Creek Gas Processing Facility (Wyoming, USA): ExxonMobil, ChevronTexaco, and Anadarko Petroleum Corporation use a pre-combustion capture method to recover around 7 million tons of CO_2 per year from natural gas production. This captured CO_2 is then used nearby for enhanced oil recovery.
- Boundary Dam CCS Project (Saskatchewan, Canada): SaskPower began installation of a post-combustion CO_2 capture project on a 110 MW coal power plant. The captured CO_2 will be utilized in the nearby Weyburn field for Enahanced Oil Recovery.
- Enhanced Geothermal System at Soultz (France): The European Union has funded an R&D project in the Soultz region of France to further the development of EGS. Currently the 1.5MW plant has been connected to the grid and is used to study the connections of multiple stimulated regions and the performance of the production wells over time.

Chapter 2

The Usage of CO_2 in EGR and EGS

2.1 Brief Description of Supercritical CO_2 and its Properties

In order to properly implement CCUS technologies into the emerging markets of EGR and EGS, it is important to understand the chemical and thermodynamic properties of CO_2. A Carbon dioxide molecule consists of a double covalent bond between one carbon atom and two oxygen atoms. It has an atomic weight of 44.01 g/mol. As seen in the phase diagram of CO_2 in Figure 2.1, CO_2 becomes supercritical above a temperature of 31°C and pressure above 72.8 atm or 73.8 bar. While at standard atmospheric temperature and pressure, CO_2 behaves like a gas; in its supercritical phase CO_2 adopts properties of both a gas and a liquid. Supercritical CO_2 typically has a density close to that of a liquid but viscosity and diffusivity similar to that of a gas.

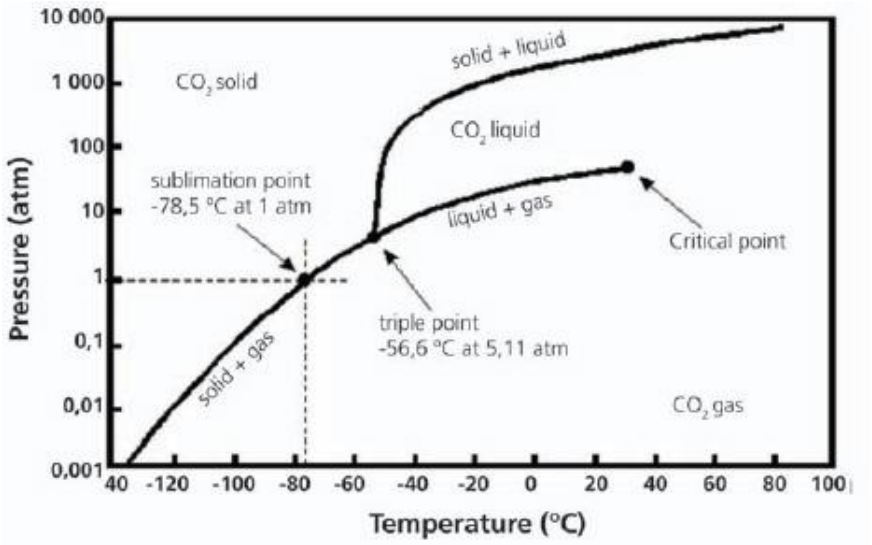

Figure 2.1: Phase transition diagram of CO_2 [12]

The physical properties of CO_2 vary widely depending upon the temperature and pressure of the system. Figures 2.2 and 2.3 respectively show the changes of mobility and enthalpy for CO_2 with change in temperature and pressure; these figures also compare these properties with that of water.

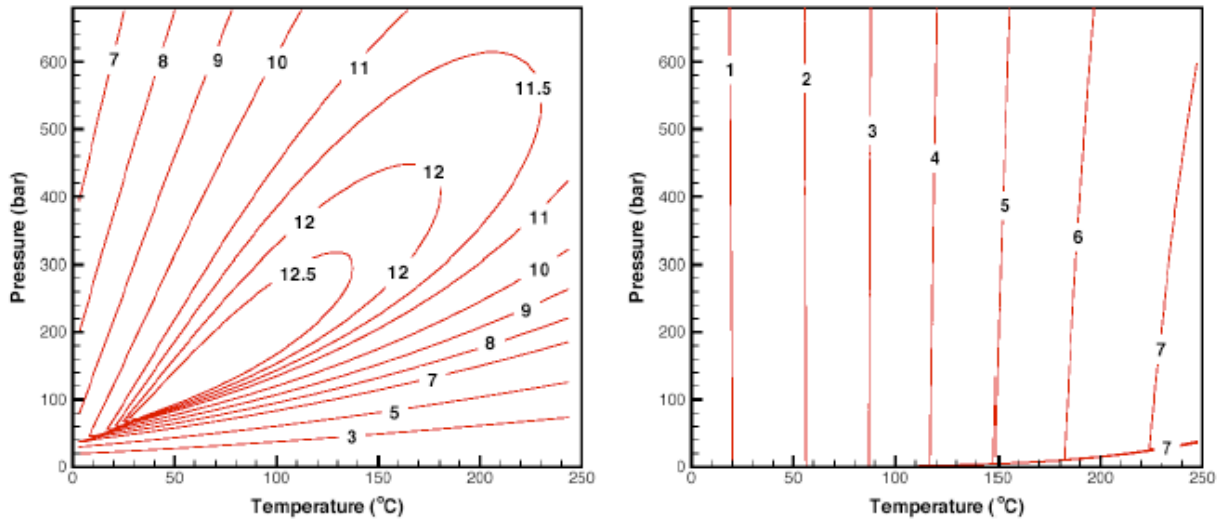

Figure 2.2: Mobility of CO_2 (left) and water (right) in units of 10^6 sm^{-2} [13]

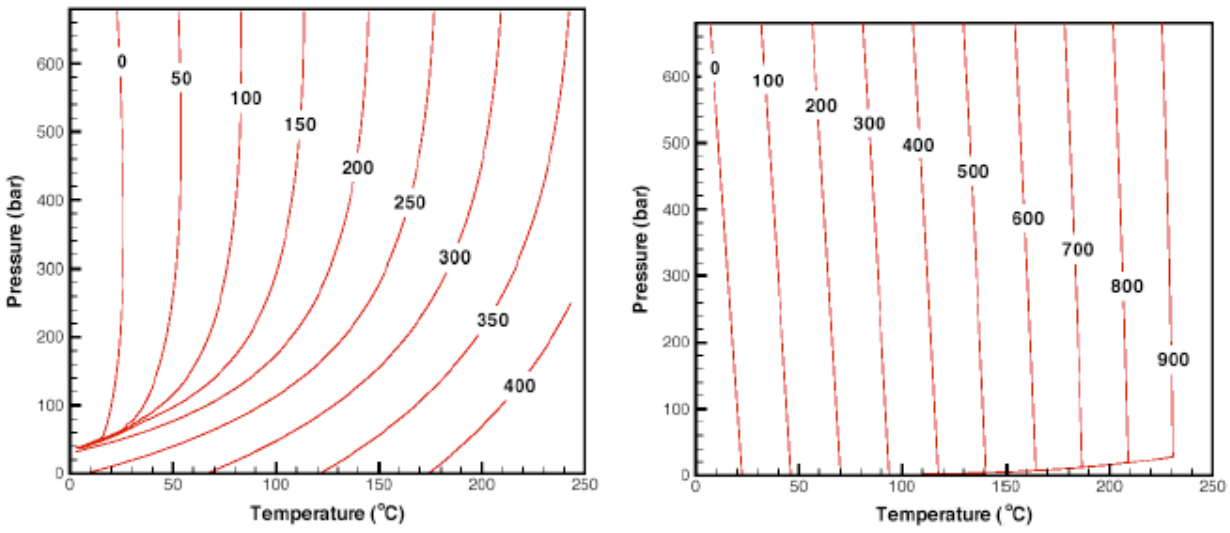

Figure 2.3 Enthalpy of CO_2 (left) and water (right) in units of KJ/kg [13]

From Figure 2.2 it can be seen that CO_2 mobility varies significantly depending on the pressure and temperature. However for water the mobility varies with change in temperature but it is almost independent of changes in pressure. Similarly for relative enthalpy, CO_2 enthalpy varies significantly with changes in both temperature and pressure whereas water's enthalpy changes primarily with temperature and not significantly with pressure.

Utilization of CO_2 in an EGR system normally occurs at elevated temperature and pressure levels depending on the characteristics of the natural gas reservoir to be replenished. Natural gas reservoirs generally exist at depths between 1 and 5km. With a pressure gradient of approximately 100 bars/km and a temperature gradient of approximately 25°C/km, it is expected that EGR is likely occur in the supercritical region of Carbon Dioxide. For EGS, the general consensus is to utilize supercritical CO_2 as a heat transmission fluid. Thus, in order to take advantage of supercritical CO_2's high mobility, the reservoir conditions must be above 73.8 bar and 31°C.

2.2 EGR/EGS Modeling Considerations

In EGR systems the predominant reservoir fluid is methane; however additional brine or aqueous solutions may be present. It is expected that there will be complex interactions between methane and carbon dioxide as well as interactions between the reservoir fluids and the surrounding rocks. As a result, it is essential to consider the dynamics of multi-component, multi-phase flow in modeling and simulation of EGR. In EGS under consideration brine and other aqueous mixtures are present at the beginning of reservoir development. While their mass fractions diminish as a CO_2 flow path is established through the reservoir, it is very likely that small amounts of water and brine will exist for

the life of the system. The interaction of CO_2 with brine and other aqueous mixtures, and minerals again requires a multi-component, multi-phase flow solver for numerical modeling and simulations.

For both EGR and EGS, dimensions of reservoirs can extend to kilometers in area and can be hundreds of meters in thickness. However, the CO_2 interactions with the in situ methane, brine, or minerals often occur at the microscopic level. Furthermore, the life-spans for EGR and EGS injections extend from a few years to many decades, with some trapping mechanisms extending to thousands of years. On the other end of the spectrum, some of the spatial and temporal interactions in the reservoir occur in the range of nanometers and nanoseconds. It is not feasible to account for all the spatial and temporal scales in a tractable physical model. Therefore a physical model that can accurately resolve the behavior of multi-component multi-phase flow from micro- to macro-scale in both space and time is considered.

Additional assumptions are made to simplify the model so that it can be numerically solved without intensive computational effort and cost but still provides meaningful results for industrial practice. For EGR simulations, the pertinent processes that must be accurately modeled include the migration of CO_2 through a reservoir and the resulting migration of methane out of the reservoir, as well as the injection pressure in the system. For EGS simulations, the pertinent processes that must be accurately modeled include the migration of CO_2 through the reservoir, the heat extraction through the production well, as well as the pressures in the reservoir and the interactions between the in-situ reservoir fluid and CO_2.

2.3 Selection of Multi-Component Multi-Phase Flow Field Simulation Code

Because of large physical dimensions and time period of CO_2 sequestration in industrial scale projects, it is difficult to analyze them in a laboratory or pilot scale projects. In order to simulate the effects of CO_2 injection in a large reservoir over a large time scale, Computational Fluid Dynamics (CFD) simulations provide the only alternative since field testing can be done only a posteriori. In the past three decades, CFD has been employed in many complex problems in aerodynamics, reservoir simulations, and in a multitude of other engineering applications.

In this research the CFD solver TOUGH2 (Transport Of Unsaturated Groundwater and Heat Version 2) is employed. TOUGH2 has been developed by the Earth Sciences Division at Lawrence Berkeley National Laboratory operated by the U.S. Department of Energy. It is a numerical simulator capable of modeling three-dimensional multi-phase, multi-component flows in porous or fractured media. The program was originally designed to model geothermal reservoirs, nuclear waste disposal, environmental assessment and remediation, and zone hydrology. TOUGH2 is supplied with a series of fluid property modules that allow the software to model specific cases related to many geological applications, e.g. CO_2 or N_2 in natural gas reservoirs, geothermal reservoirs with saline fluids, CO_2 sequestration in saline aquifers, as well as several other reservoir and multi-phase fluid dynamics applications. Specifically, for EGR research the EOS7C module in TOUGH2 was employed to simulate gaseous or supercritical CO_2 in natural gas reservoirs. For EGS modeling ECO2N module in TOUGH2 was employed for simulation of the transport CO_2 in gaseous, liquid, and supercritical phases into a saline fluid [14].

The TOUGH2 software has been developed on and open platform which allows other computer programs to interface with the code as well as for user enhancement for many applications. The

software consists of a series of FORTRAN 77 files which can be compiled on nearly any computer to run the executable files correctly. The TOUGH2 software in its original form does not currently have any optimization capability in it. Therefore an optimization program to run in conjunction with TOUGH2 to perform optimization studies of CO_2 sequestration and utilization has been recently developed. This optimization program is based on a genetic algorithm and the integrated program has been designated as GA-TOUGH2 [16].

2.4 Governing Equations of Multi-Component Multi-Phase Flow

In EGR and EGS applications, the flow is driven primarily by the pressure gradient between the injection and production wells. In the injection well a mass influx results in an increase in the bottom-hole pressure becoming greater than the reservoir pressure. In the production well a mass outflow results in a decrease in the bottom-hole pressure becoming less than that of the reservoir pressure. As a result of this pressure gradient a stream begins to flow through the reservoir from the injection well to the production well.

The governing multi-component, multi-phase equations of fluid dynamics for subsurface flow can be written as:

$$\frac{d}{dt}\int_{V_n} M^{\kappa} dV_n = \int_{\Gamma_n} \boldsymbol{F}^{\kappa} \cdot \boldsymbol{n} d\Gamma_n + \int_{V_n} q^{\kappa} dV_n \qquad \text{(Eq. 1)}$$

where V_n is the control volume of an arbitrary subdomain of the system, Γ_n is the closed surface that bounds the volume V_n, $\boldsymbol{n}$ is the normal vector to the surface element $d\boldsymbol{\Gamma}_{\mathrm{n}}$ pointing into the volume V_n. *M* on the Left-Hand-Side of Eq. 1 represents mass or energy accumulation per unit volume, the superscript denotes the components of mass or energy. $\boldsymbol{F}^{\kappa}$ on the Right-Hand-Side of Eq. 1

represents the net mass or energy flux through the control volume, the superscript denotes the corresponding mass or energy components. Lastly, q^{κ} represents the mass or energy source/sink within the control volume [15].

2.4.1 Mass Equation

In the context of mass conservation, the mass accumulation term in the governing Eq. 1 can be written as:

$$M^{\kappa} = \phi \sum_{\beta} S_{\beta} \rho_{\beta} X_{\beta}^{\kappa} \quad \text{(Eq. 2)}$$

where ϕ is the porosity of the media, S_{β} is the saturation of the phase β, ρ_{β} is the density of the phase β, and X_{β}^{κ} is the mass fraction of the component κ in the phase β.

The generalized form of the mass flux is also a sum over phases, it can be written as:

$$\boldsymbol{F}^{\kappa} = \sum_{\beta} \boldsymbol{F}_{\beta} X_{\beta}^{\kappa} \quad \text{(Eq. 3)}$$

Individual mass flux for each phase can be expressed by using the multi-phase version of Darcy's law:

$$\boldsymbol{F}_{\beta} = \rho_{\beta} \boldsymbol{u}_{\beta} = -k \frac{k_{r\beta} \rho_{\beta} g}{\mu_{\beta}} \left(\nabla P_{\beta} - \rho_{\beta} \boldsymbol{g} \right) \quad \text{(Eq. 4)}$$

where u_{β} is the Darcy velocity in phase β, k is the absolute permeability, $k_{r\beta}$ is the relative permeability of phase β, μ_{β} is the viscosity of phase β, $\boldsymbol{g}$ is the gravitational acceleration, and P_{β} is the fluid pressure of phase β which can be found by the sum of the pressure P of a reference phase (often the gas phase) and the capillary pressure:

$$P_\beta = P + P_{cap\beta} \quad \text{(Eq. 5)}$$

Substitution of the Eq. (2) - Eq. (4) into Eq. 1 gives the mass balance equation for multi-phase multi-component flow in a porous media [15].

2.4.2 Energy Equation

In a multiphase system, the heat portion of the accumulation term can be represented as:

$$M^\kappa = (1-\phi)\rho_R C_R T + \phi \sum_\beta S_\beta \rho_\beta u_\beta \quad \text{(Eq. 6)}$$

where κ refers to the heat component, $\rho_R$is the rock grain density, C_R is the specific heat of the rock, T is the temperature, and u_β is the specific internal energy of the phase β.

The heat flux can be summarized as the sum of conductive (first term) and convective (second term) components:

$$\boldsymbol{F^\kappa} = -\lambda \nabla T + \sum_\beta h_\beta \boldsymbol{F}_\beta \quad \text{(Eq. 7)}$$

Where κ references the heat component, λ the thermal conductivity, ∇T the temperature gradient, h_β the specific enthalpy of the phase β, and $\boldsymbol{F}_\beta$ the heat flux of the phase β.

Substituting Eq. 6 and Eq. 7 into Eq. 1, yields the energy equation of multi-phase multi-component fluid flow in a porous medium. A more detailed description of the governing equations used in the TOUGH2 software can be found in Appendix A of the TOUGH2 Manual [15].

2.5 Brief Description of Numerical Simulation Code TOUGH2

As introduced previously, TOUGH2 is a numerical program for simulating three-dimensional multi-component multi-phase flow in porous or fractured media. The mass and energy equations described in section 2.4 are used as the governing equations in TOUGH2. In order to compute the governing equations, TOUGH2 employs the integral finite difference method (IFD). In this method, the volume averages of the system are represented as:

$$\int_{V_n} M dV = V_n M_n \qquad \text{(Eq. 8)}$$

where M is the volume-normalized extensive quantity, and M_n is the average value of M over the volume V_n. The area averages in the system are represented as:

$$\int_{\Gamma_n} \boldsymbol{F}^{\kappa} \cdot \boldsymbol{n} d\Gamma = \sum_m A_{nm} F_{nm} \qquad \text{(Eq. 9)}$$

where F_{nm} is the average value of the component of $\boldsymbol{F}$ over the surface interface between volume elements V_n and V_m. Figure 2.4 gives a visual representation of the space discretization used in the IFD method. Additional information about the IFD method is given in the TOUGH2 manual. [15]

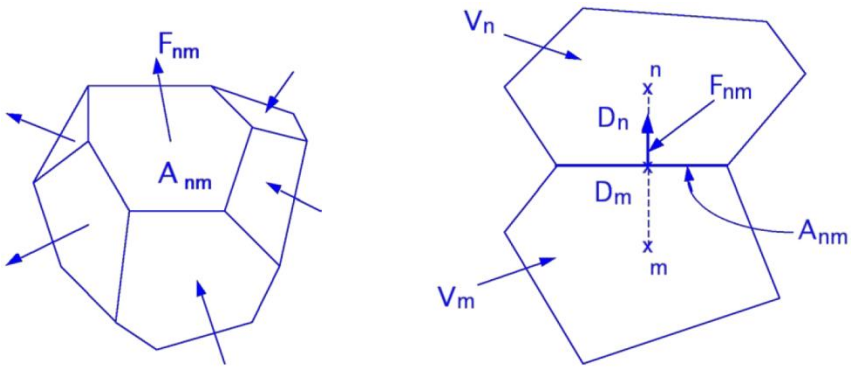

Figure 2.4: Geometric representation of IFD in TOUGH2 [15]

2.6 Brief Description of Genetic Algorithm

The Genetic algorithm is an optimization technique that mirrors natural biological evolution. The program begins with a generation of individuals modeled as a set of vectors to form an input. These individuals represent a specific sequence of data or characteristics that help to differentiate them. Each individual is then evaluated according to a fitness value determined by the user for their reproduction. A portion of the weaker individuals (those with less desirable fitness values) are deleted from the generation and the stronger individuals (those with more desirable fitness values) are kept. New offspring are produced from the characteristics of the surviving parents and then their fitness values are again evaluated. This cycle repeats for many generations and over time, much like biological evolution, an optimal individual is found. When all the individuals in a generation have similar fitness values, it implies that the genetic algorithm has converged to an optimal value. More details of the genetic algorithm can be found in reference [16]. A brief outline of the various steps in GA is given below:

1. Initialization: a series of k individuals are randomly generated which serve as the first generation.
2. Get Fitness: a fitness function or objective function value is determined for each individual in the generation.
3. Advance Generation: a new generation is created based on the individuals with the best fitness function value.
4. Replacement: a part (usually 50%) of the previous generation is replaced by the newly created off-spring; each individual fitness function is again evaluated and the process is repeated until convergence is achieved.

5. Convergence: when in a generation, all the individuals have nearly the same fitness value, convergence of GA is achieved.

The genetic algorithm is written in a java-script format and allows for easy manipulation of specific parameters such as mutation rate, individuals in a generation, natural selection rate, and fitness functions. Because of this architecture, the genetic algorithm is easy to apply to diverse optimization problems.

2.6.1 GA-TOUGH2 Integrated Program

As previously stated, the TOUGH2 software does not include an option for optimization of the performance of a problem of interest. It simply executes a single numerical simulation based on an input file and produces results in a series of output files. By using a genetic algorithm based optimizer in conjunction with TOUGH2, it is possible to create multiple input files based on a fitness function (Pre-simulation Processing), run TOUGH2 using the input files, evaluate the resulting fitness functions of all the simulations (Post-simulation Processing), and then generate new individuals based on this data. A flow chart of the integrated GA-TOUGH2 program is shown in Figure 2.5.

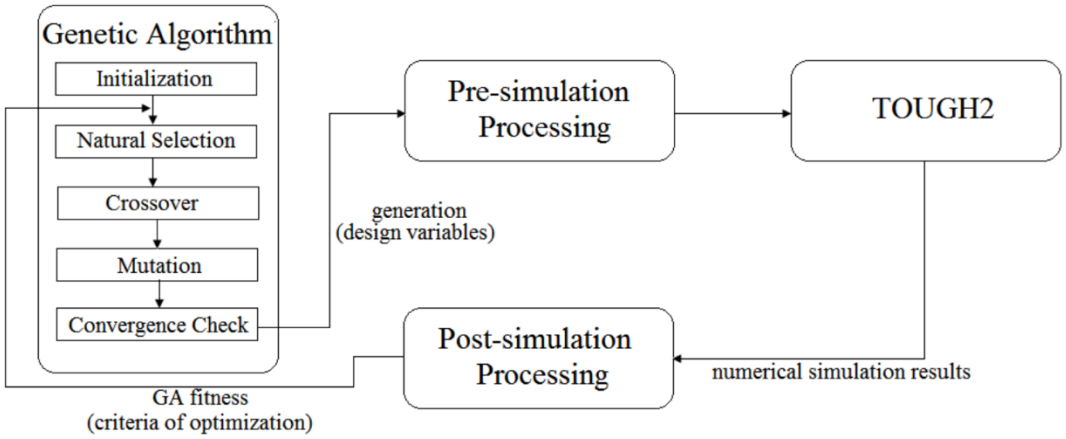

Figure 2.5: Flow chart of GA-TOUGH2 [16]

Because of the modular development of the GA-TOUGH2 code, its capabilities can be easily enhanced for a variety of applications in which multi-component multi-phase flow occurs. The code is written as a general computing platform, therefore it has the flexibility of making modifications to its existing modules or for inserting new models of permeability and porosity for example. In this thesis, the GA-TOUGH2 is used for optimization of both EGR and EGS using a time dependent and time independent injection scenario.

The TOUGH2 package consists of various source files written in Fortran77 format; the source files and appropriate modules must be compiled for execution on a specific computing platform. The TOUGH2 software does not come with any graphical user interface (GUI), all input and output files are printed in the ASCII format. While it is realtively simple to edit most of the parameters in an input file, some inputs such as mesh generation are tedious and time consuming to do without the availability of a GUI. In this research the majority of mesh generation as well as the initialization of parameters were carried out with the commercially available software PetraSim [17]. This software provides an interface to quickly generate large meshes and also allows for making quick changes to nearly all of the TOUGH2 program. In addition to serving as a visual pre- and post-processor for TOUGH2, PetraSim also provides the appropriate ASCII input files. Since PetraSim does not offer any optimization capability, the program is only used for single simulations and for generation of the appropriate TOUGH2 input file. This file is then used in conjunction with GA-TOUGH2 to optimize the specific problem of interest.

Chapter 3

Simulation and Optimization of Enhanced Gas Recovery

3.1 Model Development and Simulation of a Benchmark Problem

The TOUGH2 package was installed on a PC in the CFD lab in the department of Mechanical Engineering and Meterials Science at Washington University in St. Louis. The TOUGH2 package had prevoiusly been used in the lab for reasearch, therefore several code validation cases had already been conducted. TOUGH2 was installed on a Dell XPS 8700 PC with an 8-core Intel i7-4770 Processor at 3.40GHz, 8 GB of RAM, and a Windows 7 64-bit operating system. This machine has the necessary computational power to run complex TOUGH2 simulations and has been used in the research reported in this thesis.

Previous studies with TOUGH2 and PetraSim software produced identical results and thus PetraSim was validated as an accurate interface for use with TOUGH2 [16]. In addition, previous code validation studies with TOUGH2 were performed on three widely used benchmark problems in the CFD lab. These benchmark problems were part of a Workshop on Numerical Models for Carbon Dioxide Storage in Geological Formations at the University of Stuttgart, Germany [5]. While all three benchmark problems are related to CO_2 storage, of specific interest in this research is the benchmark problem #2. A recent update to the PetraSim software allows the implementation of the EOS7C module of TOUGH2 which is used for the simulation of benchmark problem #2 studied in this section [17].

This problem focuses on the both the total amount of CH_4 that can be extracted from the reservoir through the injection of CO_2, as well as on the storage of CO_2 in the depleted reservoir. Depleted natural gas reservoirs are considered to be one of the prime candidates for long term storage of CO_2 since they have the inherent capability of storing light gases for long periods of time. It has been recently suggested that the injected CO_2 would displace a significant amount of natural gas in the reservoir which has not been econimical to extract in the past [18]. From a logistical standpoint, much of the infrastructure needed for enhanced gas recovery is already present at the site. The focus of current EGR projects is to re-energize a depleated or depleating natural gas reservoir in order to extract the remaining gas inside the reservoir [18]. Many suitable injection and production wells are likely already present at the reservoir site due to prior gas extractions. The benchmark problem #2 is considered in this research to explore the viability of EGR with CO_2 injection.

The numerical model for benchmark problem #2 follows the common five-spot injection/ production pattern. It consists of a central injection well surrounded by 4 production wells, as shown schematically in Figure 3.1. Because of the symmetry of the five-spot pattern, only one-fourth of the reservoir needs to be modeled. The hydrogeological properties of this reservoir are given in Table 3.1.

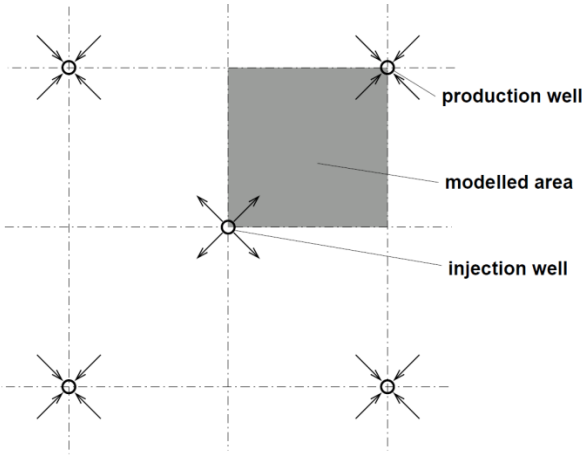

Figure 3.1: Geometric Sketch of the five-spot injection/production wells

Table 3.1: Geometric and hydrogeological properties for benchmark problem #2

Dimensions of quarter five-spot domain	201.19m x 201.19m
Reservoir thickness	45.72m
Porosity	0.23
Brine saturation	0
Reservoir temperature	66.7C
Initial reservoir pressure	35.5 bar
Coefficient of molecular diffusion	6×10^{-7} m^2/s
Horizontal permeability	50×10^{-15} m^2
Vertical permeability	5×10^{-15} m^2
Boundary conditions	No mass flow at boundaries, constant conditions at production well
Initial CO_2 mass fraction	$X_{CO2} = 0$
Initial CH_4 mass fraction	$X_{CH4} = 1$

The computational domain is discretized into 10 layers each with a thickness of 4.572 m. The injection of CO_2 into the reservoir occurs in the lowest layer at 0.4kg/sec (0.1 kg/sec for the quarter five-spot domain) and the production occurs at the opposite corner in the highest layer. This setup is employed to avoid substantial gas mixing of the CO_2 and CH_4 and ensures a better sweep efficiency of CO_2 through the reservoir. The remaining parameters to complete the input file for TOUGH2 are left to the user to fill, and often default values are used. The simulation is terminated when there is 20% (by mass) CO_2 contamination in the production stream signifying a substantial CO_2 outflow from the production well. The production well shut-in time corresponds to this break-through condition.

At the well shut-in time the total gas recovery factor of the reservoir is calculated by the formula:

$$Recovery\ Factor = \frac{Mass\ of\ CH_4\ Recovered}{Inital\ Mass\ of\ CH_4}$$

3.1.1 Comparisons of Numerical Simulations for Benchmark Problem #2

A simulation was performed on benchmark problem #2 and the present results are compared with those of other investigators. These comparisons are described in this section. Figure 3.2 compares the results using TOUGH2 and module EOS7C (exterior graph in blue and red) with those of other investigators presented at the Stuttgart Workshop (inset figure). Table 3.2 compares the recovery factor and well shut-in time of the other investigators and the results obtained in this study.

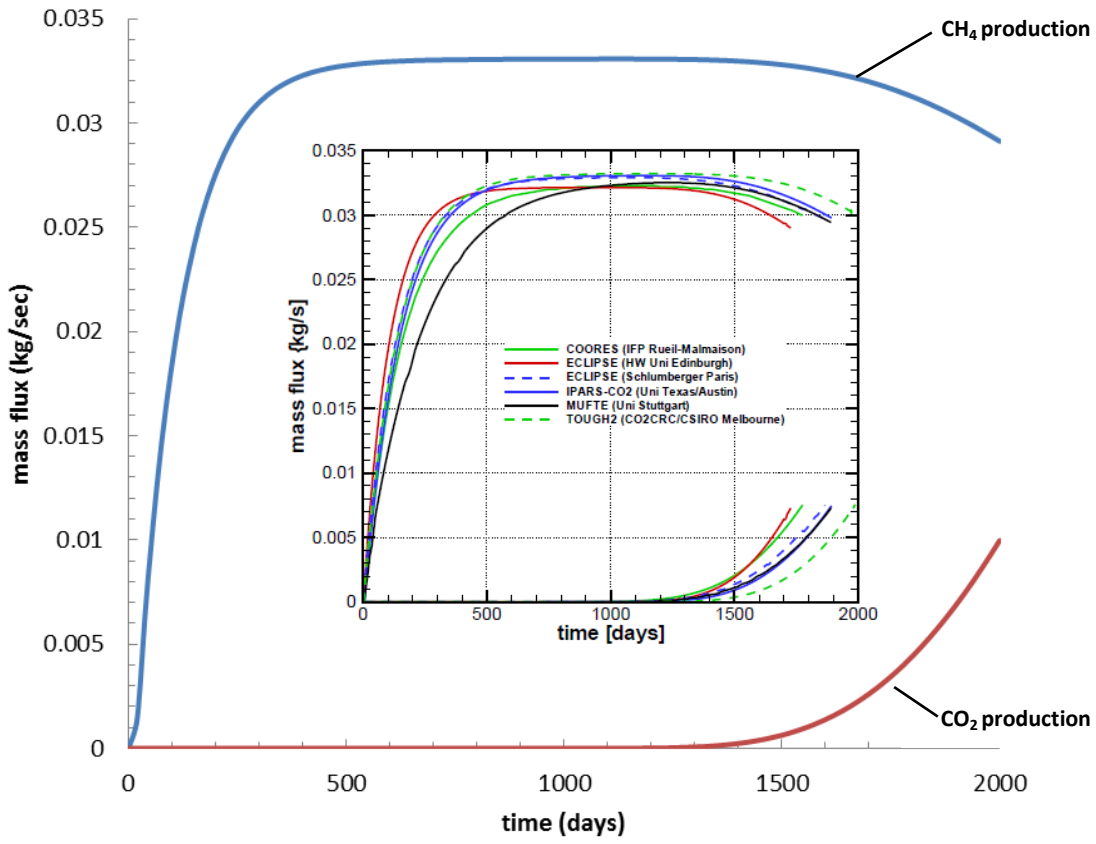

Figure 3.2: Comparison of WUSTL results (exterior graphs in blue and red) with those of other researchers (inset figure)

Table 3.2: Comparison of recovery factor and production well shut-in time

Computational code used	Recovery factor (%)	Production well shut-in time (days)
COORES	49	1775
ECLIPSE (Heriot-Watt)	50	1727
ECLIPSE (Schlumberger)	54	1865
IPARS-CO2 (U. Texas Austin)	55	1891
MUFTE (U.Stuttgart)	53	1894
TOUGH2/EOS7C (CO2CRC/CSIRO)	58	1987
TOUGH2/EOS7C (WUSTL-Biagi)	57.5	1922

Figure 3.2 and Table 3.2 show some differences among the results obtained by various researchers using different computational codes. These differences can be attributed to the numerical model used in different codes as well as the user-defined additional parameters chosen by the various researchers. The present results of the WUSTL-Biagi using the TOUGH2/EOS7C module are generally in good agreement with the results from the other codes. This simulation validates the accuracy of the WUSTL-Biagi model which is employed for the optimization study reported in the next section.

3.2 Optimization of the Benchmark EGR Problem

The benchmark problem discussed in section 3.1 serves as a simple example of an EGR scenario. It attempts to quantify both the extraction of CH_4 and the CO_2 storage in order to provide an accurate estimate on the recovery of CH_4. In order to provide an economic incentive for the implementation

of EGR systems in industry it is necessary to increase the recovery factor and decrease the well shut-in time. Increasing the recovery factor will increase the amount of natural gas that can be sold for a profit and increase incoming revenue for the industry. By decreasing the well shut-in time, the cost of well operation will decrease thereby lowering the cost of extraction.

In order to determine the optimal recovery factor for natural gas extraction for the benchmark EGR problem, this research employs the GA-TOUGH2 code. The GA-TOUGH2 code will be used first to optimize the recovery factor for a constant mass-rate injection of CO_2. Later, it will be used to optimize a time-dependent injection scenario for CO_2 to maintain a constant pressure in the injection well.

3.2.1 Optimization of Recovery Factor for a Constant Injection Rate

Before an optimization can conducted on the benchmark EGR problem, a few key parameters must be determined by performing a series of TOUGH2 simulations at different injection rates. For this study the reservoir conditions of the benchmark problem #2 described in section 3.1 are kept the same, however the injection rate is varied at specified increments. Because of the low permeability and geometric parameters of the reservoir it is not expected that an optimal value of injection rate will be greater than 0.5 kg/sec. Rates higher than 0.5 kg/sec will result in substantial pressure increase in the reservoir which may cause reservoir fracture and an unstable injection. A lower threshold for the injection rate was established at 0.1 kg/sec based on parameters of the benchmark problem discussed in section 3.1. Thus, an additional injection rate was selected between the higher (0.5 kg/sec) and lower (0.1 kg/sec) bounds to obtain insight into the effect of change in the injection rate. These three "brute-force" simulations are used to compare with the optimization results from GA-TOUGH2. Figures 3.3 and 3.4 are produced to determine what to expect from the reservoir optimization.

Figure 3.3 shows the effect of increasing injection rate on the recovery factor of the reservoir. Increasing the injection rate from 0.1 kg/sec to 0.3 kg/sec improves the recovery factor by approximately 5.8%. Another increase in injection rate to 0.5 kg/sec however reduces the recovery factor by approximately 5.5%. This supports the belief that there is a maximum value for the recovery factor between injection rates of 0.1 and 0.5 kg/sec.

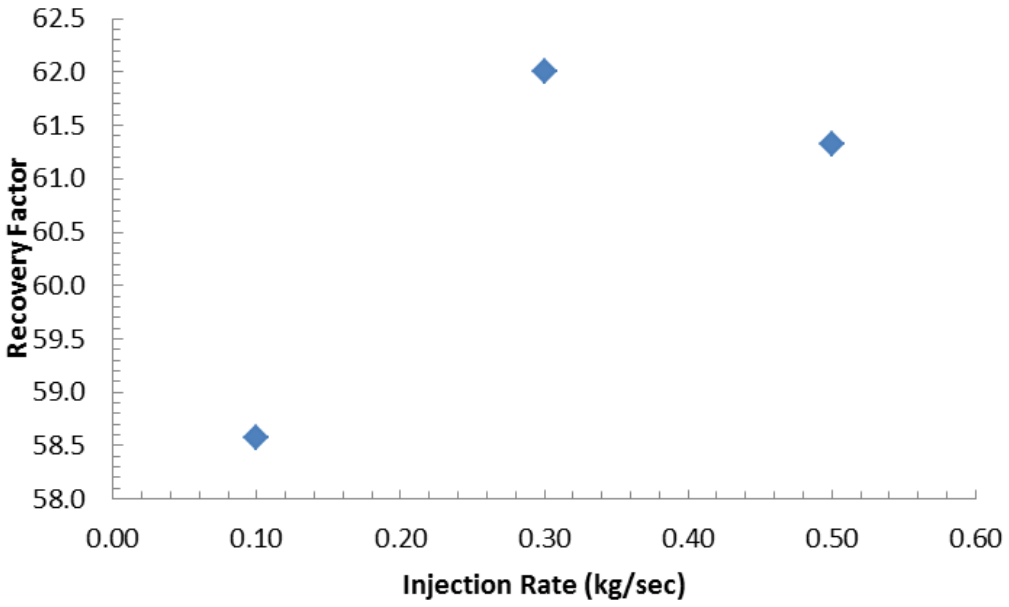

Figure 3.3: Recovery factors at well shut-in for three "brute force" injection rates

Figure 3.4 shows a plot of simulation time in days and the amount of CO_2 contamination in the production stream. The thick red line marks the point of "well shut-in" which occurs with 20% (by mass) CO_2 contamination in the production stream. From this figure it can be seen that the higher injection rates have a significantly shorter life cycle than the base case 0.1 kg/sec injection rate. This explains why the 0.5 kg/sec injection rate has a lower recovery factor than the 0.3 kg/sec rate. The higher injection has a quicker CO_2 contamination and thus well shut-in occurs at an earlier time. A

shorter well life will lead to a lower operational cost and thus the optimization should try to achieve a quick well shut-in time, with a large recovery factor.

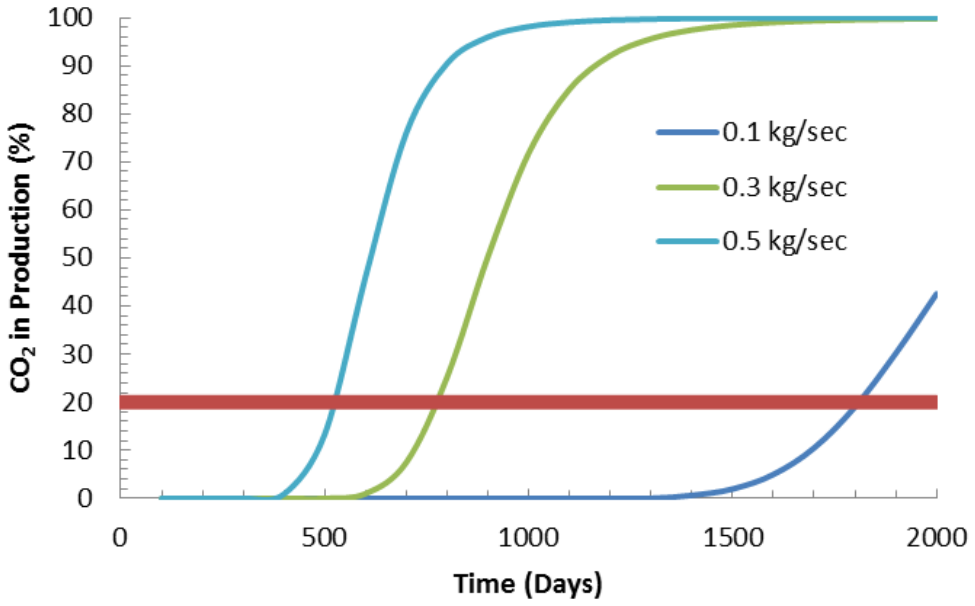

Figure 3.4: Mass percentage of CO_2 in production stream (Thick red line denotes well shut-in condition)

Figure 3.5 shows the production efficiency against the total simulation time. It is determined by the relation:

$$Production\ Efficency = \frac{Mass\ of\ Methane\ Produced}{Mass\ of\ CO_2\ Injected}$$

The three injection rate cases in Figure 3.5 have very similar curves for their production efficiency up until their respective well shut-in time. After the well shut-in, there is little methane produced for the amount of CO_2 injected. Comparing Figure 3.5 to Figure 3.4 this relationship can be clearly noted. For 0.5 kg/sec injection rate, 20% CO_2 contamination occurs in approximately 520 days, and

as expected the production efficiency begins to fall off at this point. For 0.3 kg/sec and 0.1 kg/sec injection rates, 20% CO_2 contamination occurs as well as production efficiency decreases in about 750 and 1820 days respectively. Figure 3.5 is important to describe the rationale behind the decision to close the production well at 20% CO_2 contamination. At this stage of extraction there is no longer enough methane produced to warrant continued CO_2 injection.

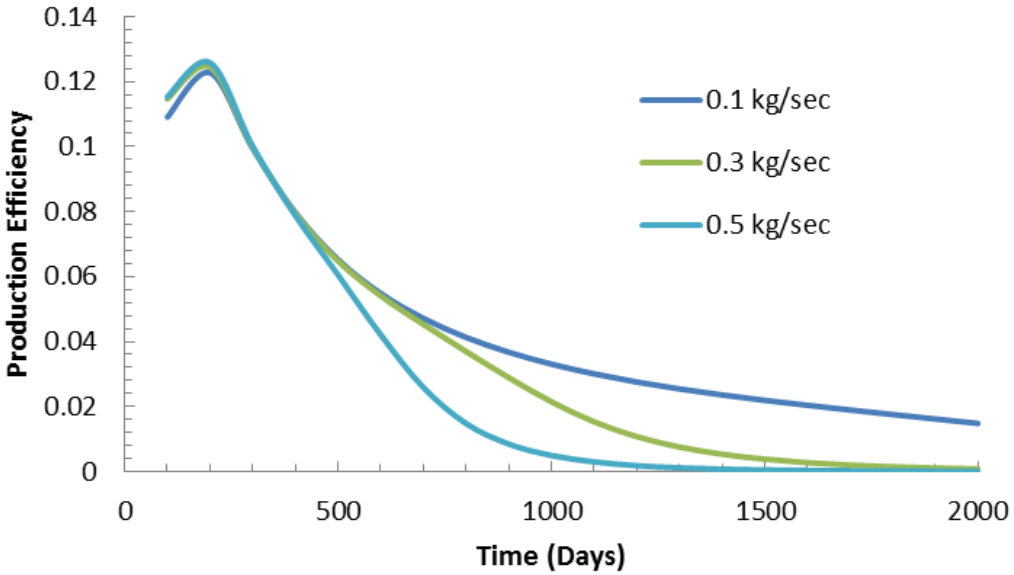

Figure 3.5: Production efficiency of CH_4 production

The fracture pressure of a reservoir is the pressure at which the rock in the reservoir can be fractured; it can therefore change the porosity and permeability of the rock. The threshold pressure in the reservoir is therefore kept well below the fracture pressure. In the 5-spot model of Figure 3.1, the highest pressure is in the injection cell and in the cells adjacent to it. The pressure of the injection cell is monitored using the FOFT output file of TOUGH2. FOFT is an optional output file that provides the time dependent characteristics of a computational cell in the domain. The FOFT is organized such that at a given time step number, it provides time, pressure, temperature, brine mass concentration, CO_2 mass concentration, water mass fraction, and CH_4 mass concentration for a computational cell in the domain [15]. Using this data one can generate the pressure profile for a specific injection cell as shown in Figure 3.6. Given the initial reservoir pressure of 35.5 bar, a 120% overpressure threshold is approximately 42.6 bar.

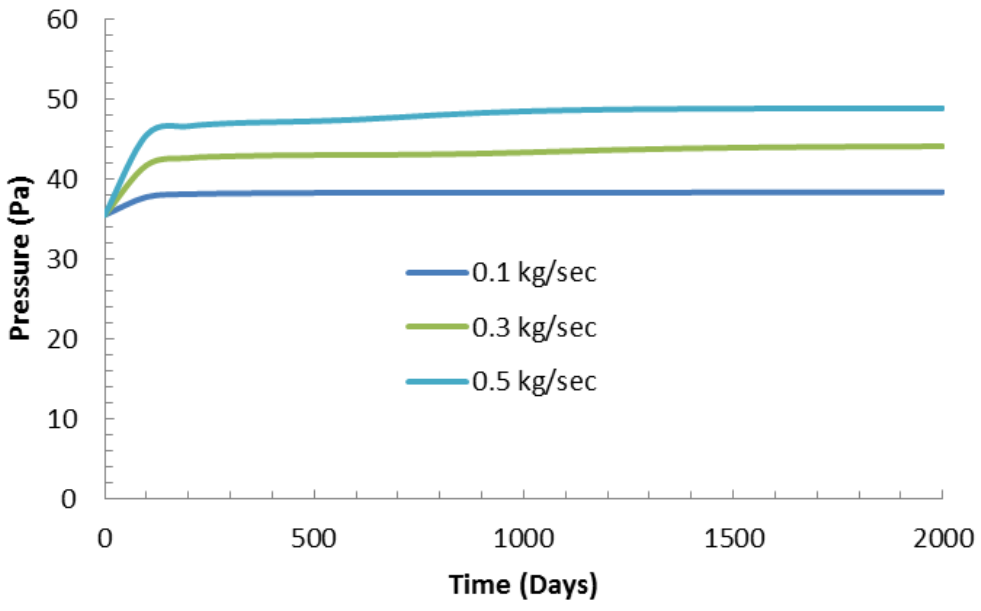

Figure 3.6: Injection cell pressure

As can be seen from Figure 3.6, the injection cell pressure for an injection rate of 0.1 kg/sec is well below this threshold, for injection rate of 0.3 kg/sec reaches steady state pressure close to 44 bar, and for injection rate of 0.5 kg/sec reaches steady pressure close to 48.8 bar. Thus we can conclude that the low injection rate will have no possibility of rock fracture, the mid injection rate may will have some possibility of mainly fracture near the injection cell; however the high injection rate may result in reservoir fracture. The control of injection cell pressure is analyzed in a later section.

As mentioned before, in a CSEGR system with low injection rates there is very limited mixing between the injected CO_2 and the in-situ CH_4 [19]. A low injection rate will ensure that CO_2 migrates through the reservoir as a plume and will not spread in an irregular fashion due to diffusion or high pressures. A low injection rate also means a low production rate of CH_4 by simple displacement within the reservoir. On the other hand, a higher injection rate of CO_2 will lead to a higher production rate of CH_4, but it may reduce the life expectancy of the extraction. The larger injection rates of CO_2 can cause a separation of the plume and can lead to a premature break-through at the production well. This implies that there should be an optimum value of the CO_2 injection rate between the high and low injection rate that allows for a relatively higher injection rate, but also a low CO_2 contamination.

Since each injection rate results in a different CO_2 migration pattern, one cannot rely on one specific time measurement for the calculation of the recovery factor. The concentration of CO_2 can be continuously monitored in the production cell of the reservoir through the use of the corresponding TOUGH2 FOFT file. At the appropriate time step of well shut-in (corresponding to a 20% by mass contamination of CO_2 in the production stream), the approximate recovery factor of the well can be determined and the resulting fitness function can be calculated in GA-TOUGH2. Parameters for this GA-TOUGH2 case are organized in Table 3.3.

Table 3.3: GA-TOUGH2 parameters

Individuals per Generation	6
Maximum Number of Generations	50
Natural Selection Algorithm	50%
Mutation Rate	8%
Cross-Over Algorithm	Semi-Random Combination of Parents

From Figure 3.7 it can be seen that GA-TOUGH2 achieves convergence after approximately 5 generations. GA-TOUGH2's best individual is also shown in this figure. In Figure 3.8, the recovery factor based on optimal injection rate from GA-TOUGH2 is superimposed on three recovery factors obtained from standard TOUGH2 simulations for injection rates of 0.1 kg/sec, 0.3 kg/sec, and 0.5 kg/sec.

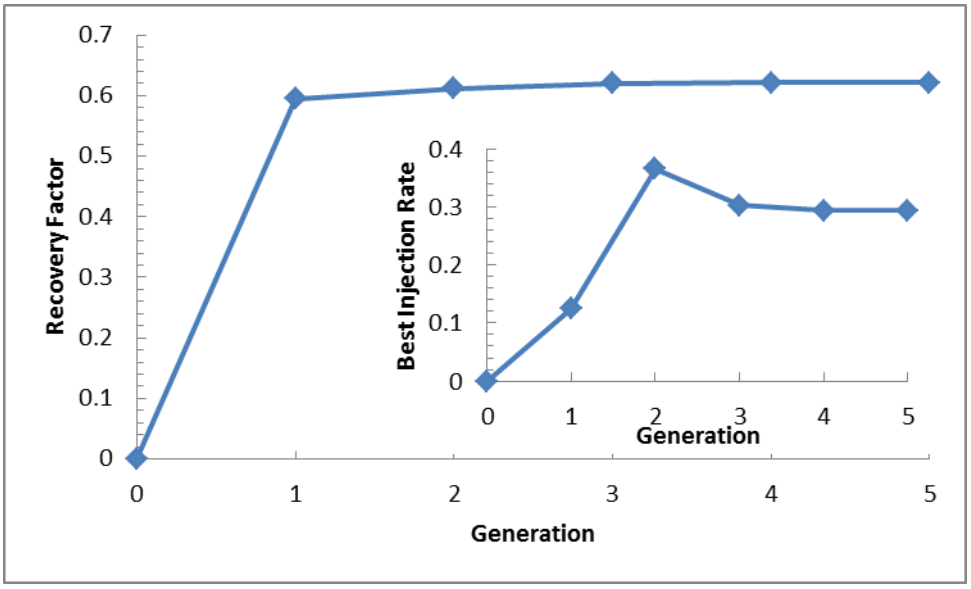

Figure 3.7: GA convergence history and injection rates

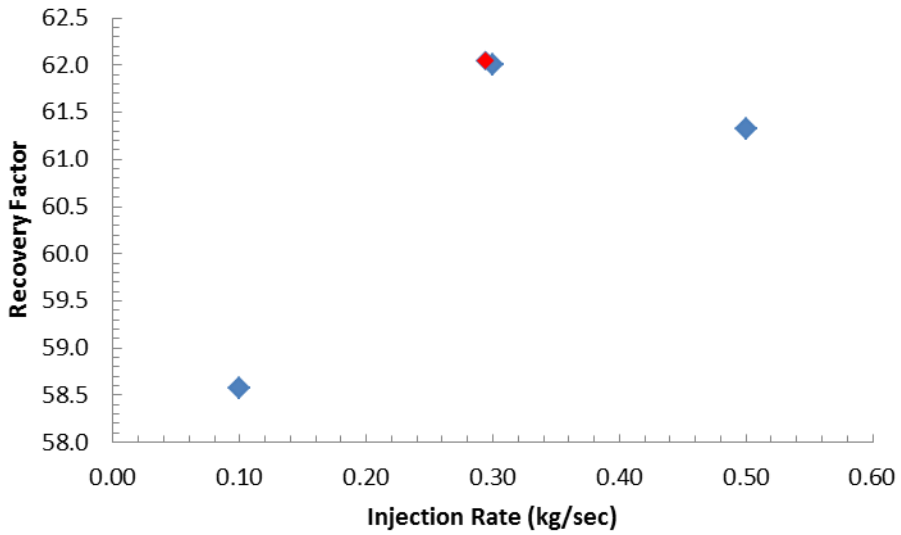

Figure 3.8: Variation of recovery factor with CO_2 injection rates (optimal recovery factor shown in red)

The results of Figure 3.8 are shown in tabular form in Table 3.4, it can be seen that the GA-TOUGH2 optimum value of 0.294 kg/sec for injection rate is close to the injection rate of 0.3 kg/sec as obtained by the brute force approach. Furthermore, the recovery factor for injection rates of 0.294kg/sec and 0.3 kg/sec are nearly the same as expected. Thus, the optimal recovery will be obtained neither for very low or very high injection rates.

Table 3.4: Recovery factor comparison

Injection Rate (kg/sec)	Recovery Factor (%)	Time to Breakthrough (Days)
0.100	58.6	1960
0.300	62.0	762
0.500	61.3	494
0.294	62.1	772

For better understanding of the reservoir flow and how the CO_2 plume migrates in the reservoir, graphical representations of CO_2 mass fraction at various times from 100 days to 2000 days for base case injection rate of 0.1 kg/sec and the optimal injection rate of 0.294 kg/sec are shown in Figure 3.9. From this figure the dramatic change in the CO_2 plume migration in the reservoir with an increased injection rate can be seen. It is important to note that the sustained injections of 0.294 kg/sec past the breakthrough time (772 days) would not be continued in actual EGR operation, it is shown in Figure 3.9 for the purpose of comparison with the base case.

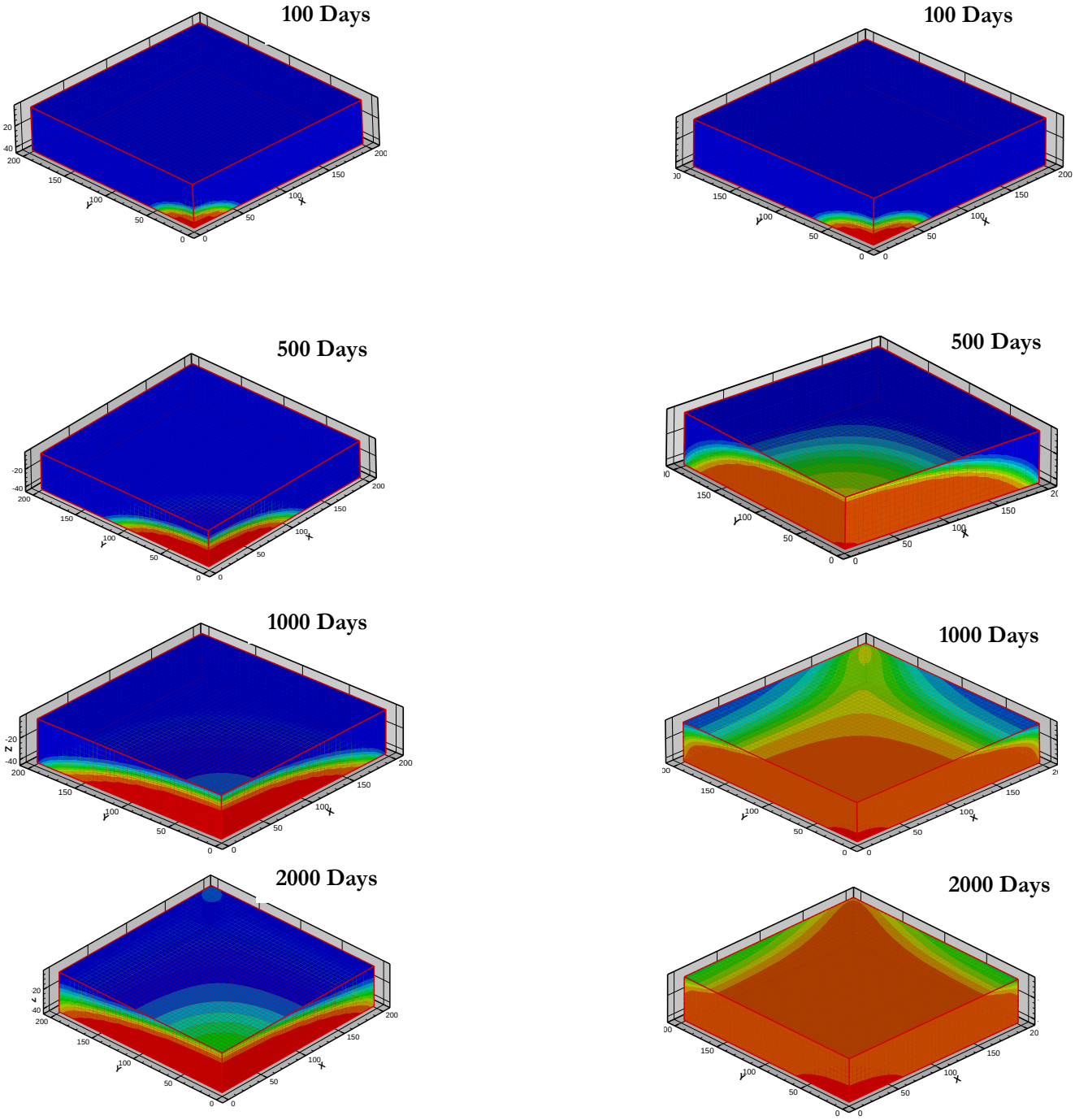

Figure 3.9: Graphical representations of CO_2 mass fraction for two injection rates (0.1 kg/sec on left, 0.294 kg/sec on right)

A comparison of methane production rate for the baseline CO_2 injection rate of 0.1 kg/sec and optimal injection rate of 0.294 kg/sec is shown in Figure 3.10. The optimal CO_2 injection rate results in a much quicker breakthrough time compared to the baseline injection rate. Furthermore, the optimal injection rate results in a higher production rate of methane and an improved recovery factor.

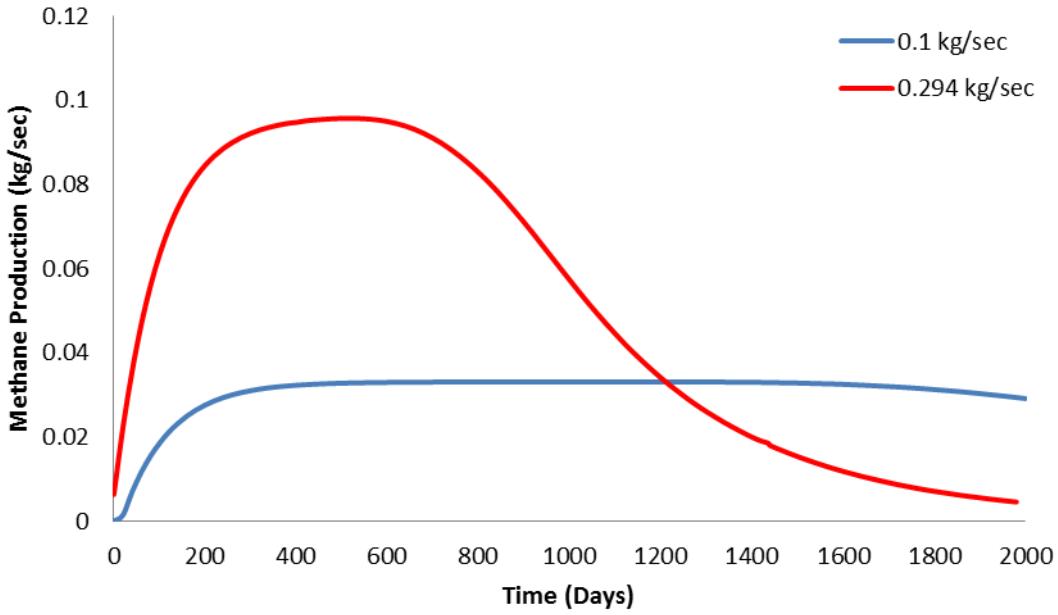

Figure 3.10: Comparison of methane production rate for the baseline (0.1 kg/sec) and optimal (0.294 kg/sec) CO_2 injection rates

Figure 3.11 shows a comparison of the injection well pressure for the optimal (0.294 kg/sec) and the base case (0.1 kg/sec) CO_2 injection rates. The pressure due to the optimal injection rate settles on a value which is over 120% of the initial reservoir pressure. While this injection rate gives an optimal value of the recovery factor, it has no control on the pressure in the reservoir. This may not be acceptable if the pressure becomes greater than the fracture pressure. Therefore a constraint on the maximum allowable reservoir pressure must be included in the optimization.

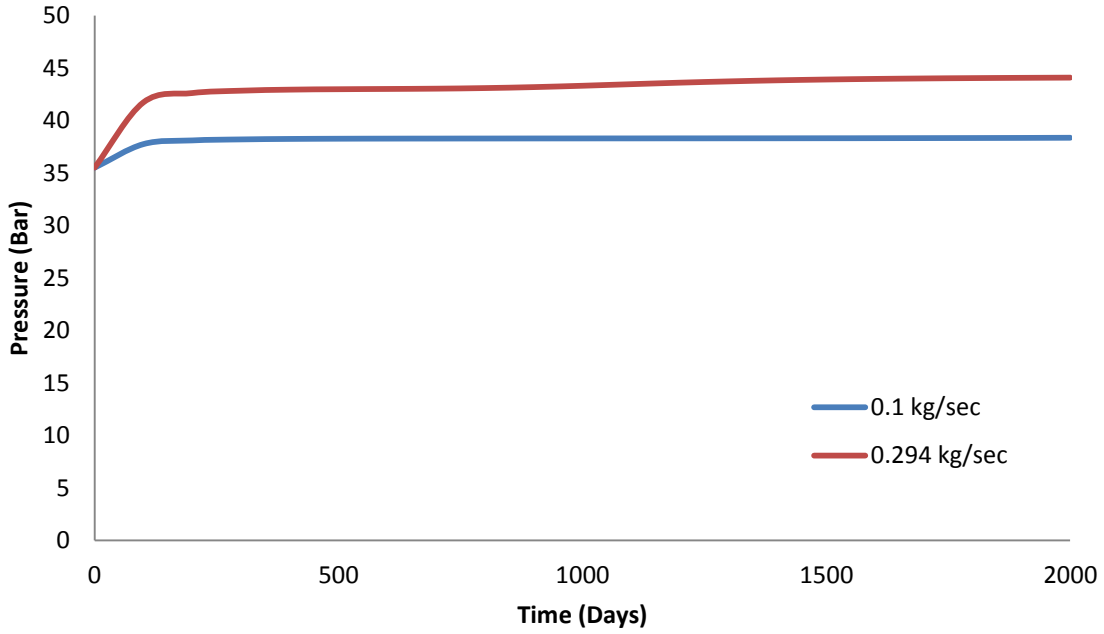

Figure 3.11: Comparison of injection cell pressure for the baseline (0.1 kg/sec) and optimal (0.294 kg/sec) CO_2 injection rates

3.3 Constant Pressure Injection (CPI) Optimization

As described in section 3.2, optimal constant injection rate obtained by GA-TOUGH2 can improve the recovery factor significantly, however it cannot control the reservoir pressure. It would not be acceptable if the reservoir pressure becomes greater than the fracture pressure. Long-term exposure to pressures in excess of the reservoir fracture pressure will result in rock fracture and a premature well shut-in. A more accurate model of the EGR process considers a time-dependent injection rate based on the injection cell pressure.

This section considers the optimization of the injection cell pressure using a time-dependent injection rate. This can be achieved by considering the well injectivity function defined as:

$$injectivity = \frac{Q_{CO2}}{P_{injection} - P_{reservoir}}$$

where Q_{CO2} refers to the injection rate of CO_2 by mass, $P_{injection}$ the injection pressure, and $P_{reservoir}$ the initial reservoir pressure. The purpose of the injectivity parameter is to determine the ability of a well to deliver CO_2 into the system. The injectivity will change with time even if the injection rate is constant, this is due to a corresponding change in the injection pressure as CO_2 migrates through the reservoir.

From Darcy's Law, it can be shown that the injection rate is proportional to the relative permeability of CO_2 as well as to the pressure gradient in the flow region. At the beginning stage of EGR operation, the majority of the reservoir and cells near the injection well are filled with methane. The displacement of this in-situ methane results in a large initial increase in the injection pressure. Once the flow develops in the reservoir, and a large amount of mass flow goes out of the reservoir through the production well the pressure begins to stabilize towards a constant value. This is due to low CO_2 injectivity at the beginning of injection and high CO_2 injectivity in later stages of EGR operation. This phenomena can be explained by the use Figure 3.12 below. Regardless of the injection rate, the variation in pressure with time follows a similar format, rapidly increasing in early stages and then slowly decaying as time increases and as CO_2 displaces more and more CH_4 and increases its relative permeability.

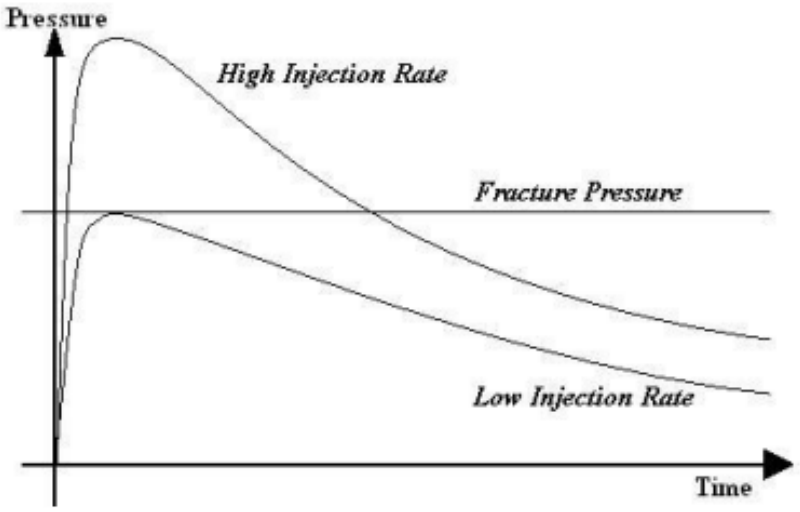

Figure 3.12: A schematic showing the variation of injection pressure with time for constant mass injection rates

In most cases a high injection rate of CO_2 is desirable as it leads to a high production rate of CH_4 as was shown in section 3.2. However, a higher injection rate can result in a much greater injection pressure, which may exceed the fracture pressure of the rock. All geological formations have a limit on the allowable pressure for maintaining their structural integrity. While this limit varies from formation to formation and changes with reservoir depth; for a specific reservoir one can assume that the fracture pressure is the same throughout the reservoir and will remain the same during the life of its use. Thus a constant horizontal line is drawn in Figure 3.12 for the fracture pressure of the reservoir. Exceeding the fracture pressure and lead to harmful consequences, in particular rock fractures may result in CO_2 migration into the other surrounding structures such as water aquifers, and potentially all the way to the surface. Thus, an injection resulting in reservoir pressure in excess of the rock fracture pressure must be avoided.

The primary technique to control the injection pressure is to employ a constant pressure injection. The mass injection rate is varied with time such that the injection well pressure does not exceed the

allowable limit. The time dependent mass injection scenario opens the door for utilization of another optimization technique. An ideal injection profile would reach the allowable reservoir pressure very quickly and would then maintain this pressure throughout the life of the injection. This procedure would combine the quick rise to pressure as seen in a constant high injection rate with the lower lifetime injection pressure of a constant low injection rate as shown in Figure 3.12. In addition, specifying higher injection rates in later stages of reservoir development will help mitigate the effects of the pressure decay as seen in Figure 3.12 for the constant lower injection rates of supercritical CO_2.

3.3.1 Designing the Constant Pressure Injection System

As discussed in reference [16], the optimization of a CPI system is a relatively simple extension of the original GA-TOUGH2 program [16]. A threshold pressure is chosen as an input into the program and the optimization adjusts the mass injection rate to best suit the pressure constraint. The fitness function can be defined as a slight modification to the injectivity equations:

$$Fitness\ Function = \frac{\left|P_{threshold} - P_{injection}\left(Q_{CO_2}\right)\right|}{Q_{CO_2}}$$

The fitness is defined as the difference between the threshold pressure (e.g. the fracture pressure) and the injection pressure. As this difference approaches zero, an ideal injection profile can be obtained. Although a truly zero difference may never be possible due to the time variability of the injection profile, solutions can be obtained that maintain the injection pressures within 1 bar of the threshold pressure. By taking the absolute value of the pressure difference, the injection pressure is allowed to overshoot or undershoot the threshold pressure when searching for the optimum. This leads to the present solution-searching optimization technique.

Whereas the constant mass-rate injection defined a singular time-independent function for the injection rate, the constant pressure injection seeks to define a continuous, variable, time-dependent function for the injection profile. In order to accomplish this task with relatively few design parameters, a Beziér curve is employed to define the injection profile. The Beziér curve was originally utilized to design complex curved automobile parts in the early 1960s; it is now commonly used in computer graphics and simulations [21]. A Beziér curve is constructed by the use of a series of points defined in a Cartesian coordinate system. From these few coordinate points, a path can be made to define a unique curve. The control points are typically denoted as P_0 to P_n and the order of the curve is defined as: $n-1$. The generalized mathematical equation for an nth order curve is given by:

$$B(t) = \sum_i^n \binom{n}{i} (1-t)^{n-i} t^i P_i \qquad \text{(Eq.10)}$$

In this study a cubic Beziér curve is chosen, this is a 3rd order curve dependent on 4 control points. A schematic of this curve is shown in Figure 3.13.

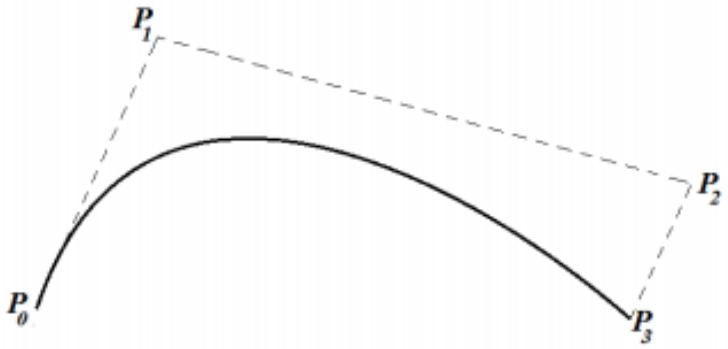

Figure 3.13: The schematic of a 3rd order Beziér curve

As defined by a previous report, the injection rate for each time step is defined by this 3rd order Beziér curve [16]. The mathematical representation of the Beziér curve can be defined in Cartesian coordinates by four control points: $P_0(x_0, y_0)$, $P_1(x_1, y_1)$, $P_2(x_2, y_2)$, and $P_3(x_3, y_3)$ where the x-axis denotes the simulation time and the y-axis denotes the injection rate [16]. For any point $P\big(x(t), y(t)\big)$ on the curve, the coordinates can be written as:

$$x(t) = A_x t^3 + B_x t^2 + C_x t + x_0$$

$$y(t) = A_y t^3 + B_y t^2 + C_y t + y_0$$

with the coefficients defined as:

$$C_x = 3 \cdot (x_1 - x_0) \qquad C_y = 3 \cdot (y_1 - y_0)$$

$$B_x = 3 \cdot (x_2 - x_1) - C_x \qquad B_y = 3 \cdot (y_2 - y_1) - C_y$$

$$A_x = x_3 - x_0 - C_x - B_x \qquad A_y = y_3 - y_0 - C_y - B_y$$

It is important to note that while the Beziér curve produces a continuous function to describe the injection rate, a continuous function cannot be implemented into the TOUGH2 input file. The GENER block in TOUGH2 allows for time dependent injection rates only at discrete time periods. To remedy this, the CO_2 injection can be discretized to become a step function for each pre-defined time interval. The injection rate is determined using the corresponding values for the midpoint of the interval or sample point. With small enough time intervals, the injection curve can closely simulate a continuously variable injection rate. The first injection rate begins at time *t = 0*, and therefore the first point can be defined as: $P_0(0, y_0)$, the other coordinates are created by GA-TOUGH2 for each individual.

The CPI optimization is very similar to that discussed previously for the constant injection rate optimization. The reservoir conditions remain the same, all physical parameters remain the same as given previously in section 3.2. However a threshold pressure is introduced as the maximum allowable injection pressure. The threshold pressure for the present case is taken as the steady-state pressure obtained for benchmark problem #2. This threshold pressure is 38.4 bar. The injection rate is allowed to vary between 0.1 kg/s and 0.5 kg/sec, and the injection proceeds for 2000 days. In order to reduce the total simulation time, the injection parameters are modeled only for the first 500 days of injection. This is an appropriate time period based on the benchmark problem #2 results to reach an almost steady pressure. The remaining injection is conducted at a slowly decaying rate down to the base case injection rate of 0.1 kg/sec. GA-TOUGH2 parameters specific to this optimization are given in Table 3.5.

Table 3.5: GA-TOUGH2 parameters for constant pressure injection (CPI)

Individuals per Generation	6
Maximum Number of Generations	50
Natural Selection Algorithm	50%
Mutation Rate	10%
Cross-Over Algorithm	Semi-Random Combination of Parents
Threshold Pressure	38.4 bar

The GA-TOUGH2 convergence history is shown in Figure 3.14. The injection profile converges to a pressure difference of 0.13 bar after 28 generations for the first 500 days. When using the same injection profile for 2000 days of injection the pressure difference was much less (0.08 bar).

Comparing these results with those for the constant injection rate of 0.1 kg/sec, the constant injection rate had an average pressure difference of 0.57 bar over the first 500 days, thus the optimized results reached the threshold pressure more quickly. The injection profile of the optimal time-dependent injection rate is shown in Figure 3.15. The injection begins at a high rate to establish an appropriate pressure in the reservoir and then quickly decays to a nearly steady state value of 0.1 kg/sec.

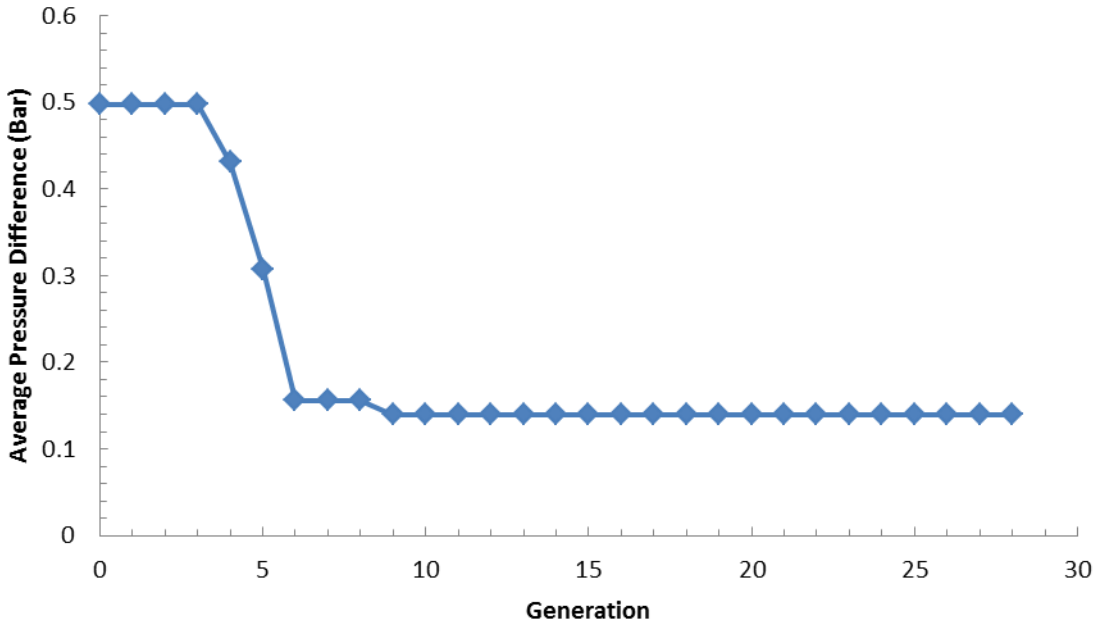

Figure 3.14: GA-TOUGH2 convergence history for a constant pressure injection case

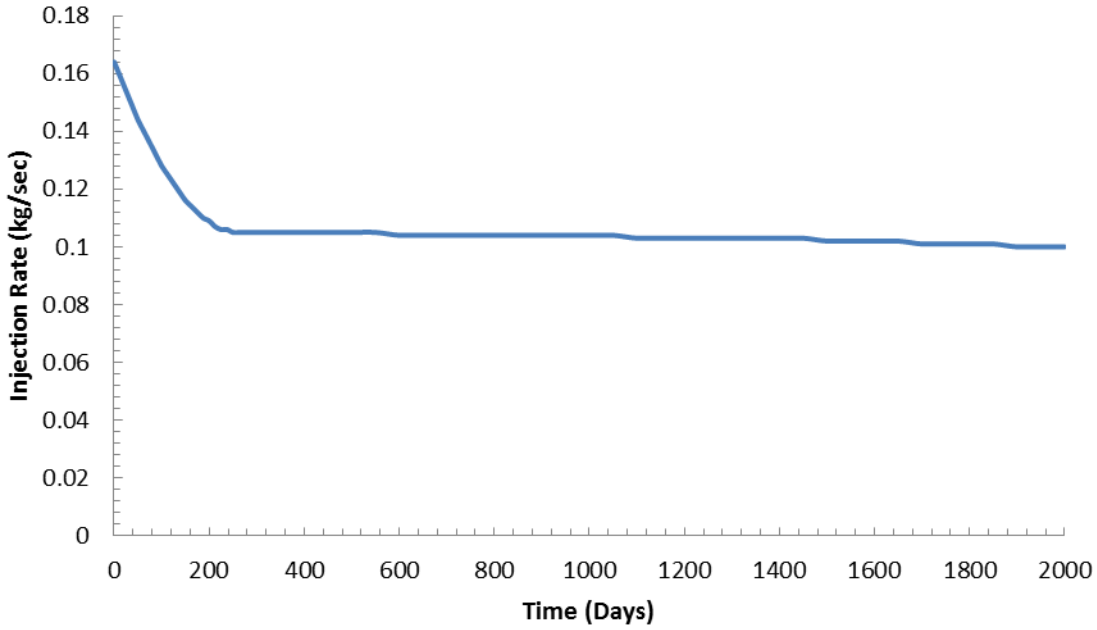

Figure 3.15 Optimal time-dependent injection profile for constant pressure injection

A comparison of injection pressures for the first 500 days and 2000 days can be seen in Figure 3.16, the result obtained from GA-TOUGH2 rises to the threshold pressure much more quickly compared to that of the constant mass rate injection.

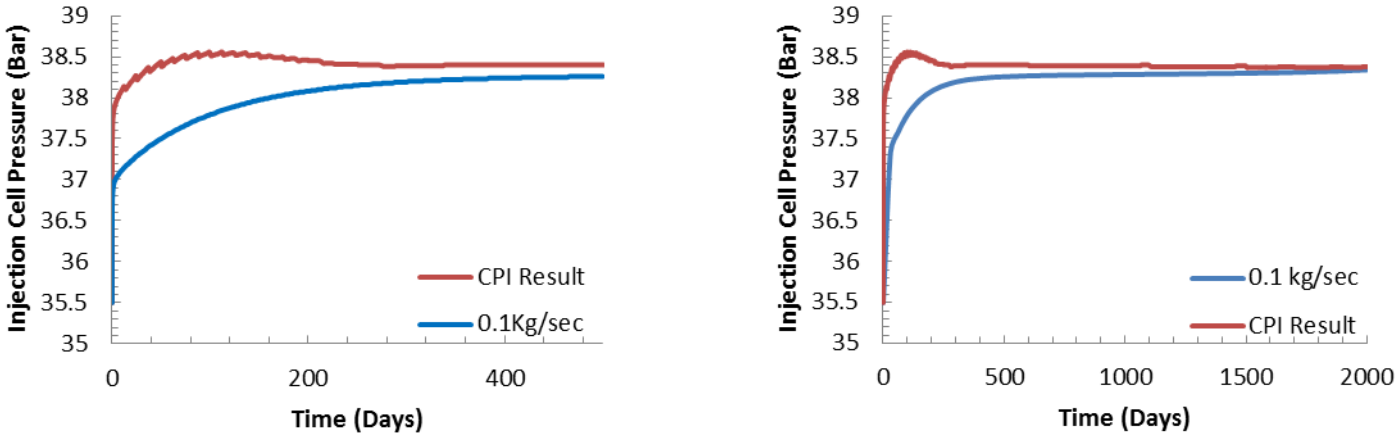

Figure 3.16: Comparison of injection cell pressures at 500 days (left) and 2000 days (right)

The combination of a slightly greater initial injection rate and a quick rise to the appropriate threshold pressure leads to quicker production of methane in the production stream. In addition, keeping the injection pressure below the threshold pressure ensures a minimum possibility of fracture and maintains safety. A comparison of methane production for constant mass injection of 0.1 kg/sec with time dependent optimal CPI is shown in Figure 3.17.

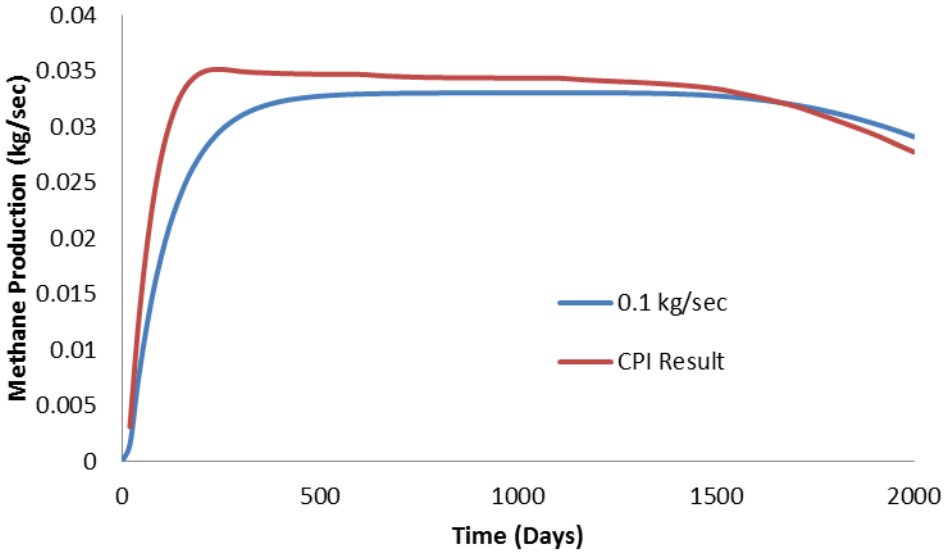

Figure 3.17: Comparison of methane production rates for constant mass injection rate and optimized CPI case

Figure 3.18 shows a comparison between the CO_2 mass concentrations in the reservoir at 100, 500, 1000, and 2000 days for constant mass injection of 0.1 kg/sec and the optimized CPI case. Initially, the constant pressure case has a larger migration of CO_2 in the reservoir, however after the threshold pressure is reached the injection rate decreases to 0.1 kg/sec. The CPI result has a higher production rate of methane and a quicker rise to the steady production rate because of the large initial CO_2 migration in the reservoir. Because the CO_2 plume is established more quickly in the optimized CPI case compared to the base case, subsequent injections have a more direct effect on the extraction of natural gas.

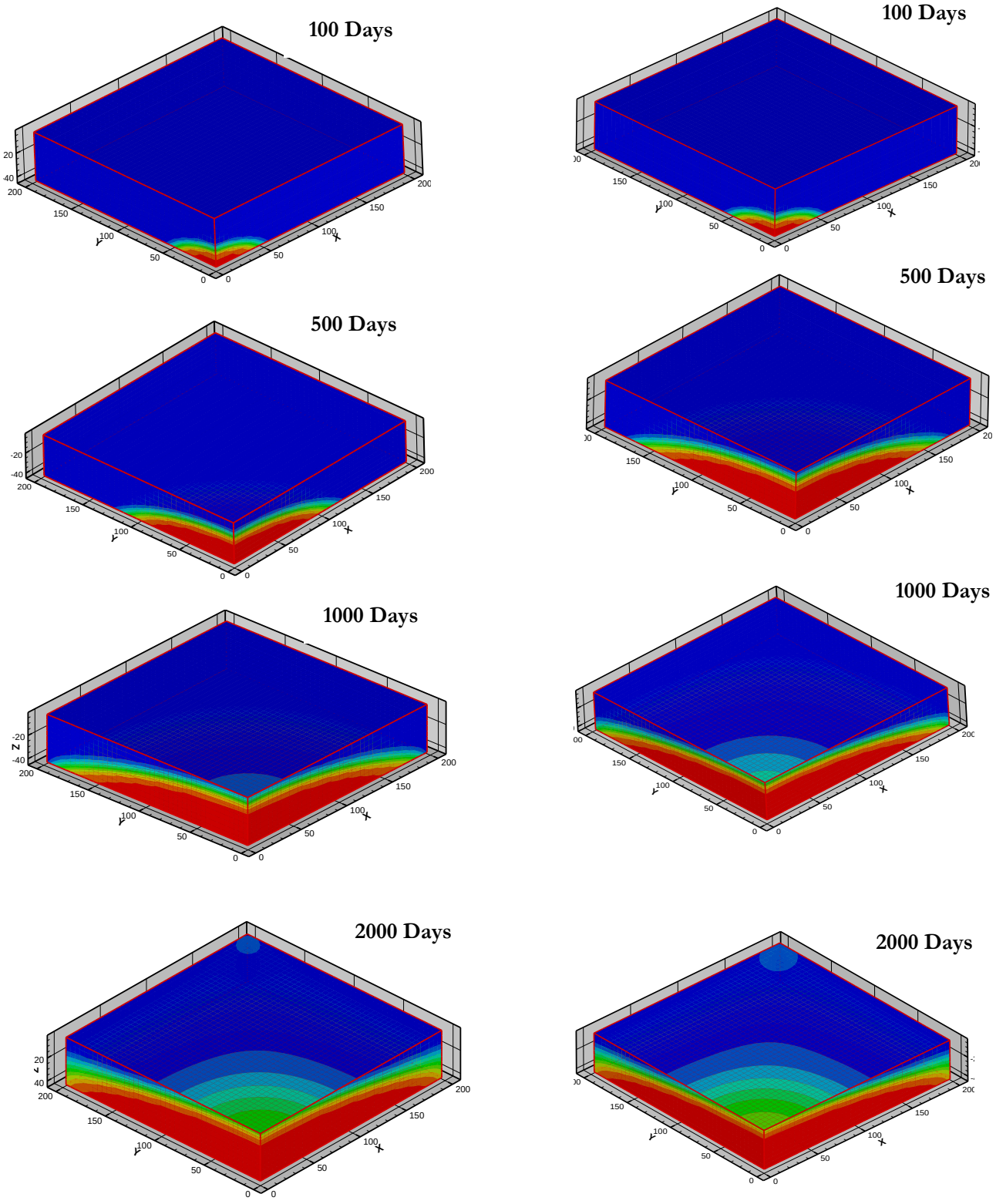

Figure 3.18: Graphical representations of CO_2 mass fraction inside the reservoir, baseline (0.1 kg/sec) (left), constant pressure injection optimization (right)

From the figures and graphical representation given for the constant pressure injection (CPI) optimization, one can see that the injection profile begins at a higher rate and reaches the threshold pressure quickly. Once the threshold pressure is established the injection profile decays to maintain the pressure within a small margin of tolerance. This pressure management leads to a higher initial methane production as well as a higher overall production during the life of the well. Although the recovery factor for the CPI and the base case are nearly the same, during the lifetime of the well, a constant pressure injection produces methane at a higher rate.

Chapter 4

Simulation and Optimization of an Enhanced Geothermal System (EGS)

4.1 Code validation of TOUGH2 software with ECO2N

Enhanced Geothermal Systems (EGS) with CO_2 as a working fluid may offer an excellent approach for simultaneously achieving the goal of clean power generation combined with geological carbon sequestration. In EGS, an existing "Hot Dry Rock" area is altered to allow for higher mass flow rates through the use of hydraulic fracturing. Once fractured, the system goes through a development phase to evacuate any residual water from the reservoir and ensure minimal water contamination in the flow stream. After the development stage, supercritical CO_2 is circulated through the system and heat is extracted from the outflow stream of CO_2 to produce power. It can be seen from the CO_2 mobility and enthalpy charts given in Chapter 2, under certain pressure and temperature conditions, the high mobility of CO_2 compared to water (although with relatively lower enthalpy compared to water) can promote significantly higher heat extraction rates than water. In developing EGS with CO_2 as a working fluid, it is imperative to maintain the thermal conditions that allow for maximum heat extraction rate. In this section an example of EGS simulation is described; the various simulations are performed at different pressures with a constant initial reservoir temperature.

The goal of the base line case chosen in this study is to replicate the results given in a previously accepted paper on EGS [21]. This paper covers a variety of topics related to EGS, of particular

interest in this work are the simulations conducted at different reservoir pressures with CO_2 and water as working fluids. A five-spot well configuration with an area of 1 km^2 and an injection-production well distance of 707.1 m is employed as shown in Figure 4.1. This geometry allows for consideration of a computational domain of only one-eighth the size of the entire domain (due to symmetry). In this study, the primary focus is on understanding the dependence of the flow behavior in the domain due to the reservoir pressure. Although only one-eighth of the domain is modeled, injection and production are assumed to occur throughout the reservoir.

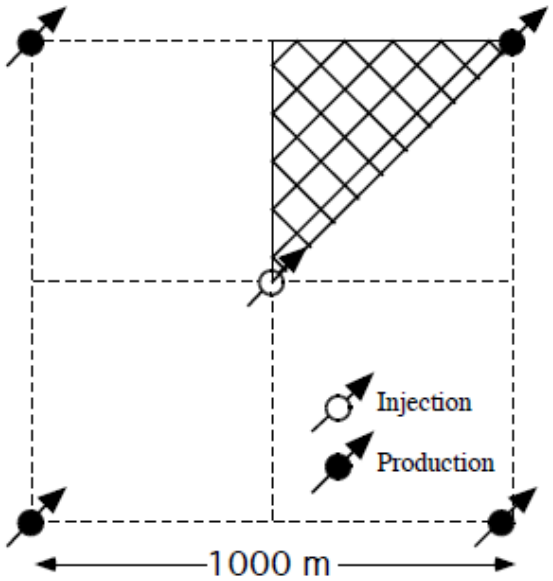

Figure 4.1: Computational domain for EGS simulations

The mesh consists of a single layer of 36 cells 305m in depth with a side length of 70.71m. The cells are oriented in a parallel alignment to the injection-production diagonal as shown in Figure 4.1. Simulations are performed using a modified high temperature version of TOUGH2 with the ECO2N module. The standard version of ECO2N has a temperature limit of 112 °C due to a lack of information about the water-CO_2 interactions above112 °C . However, when using only water or

only CO_2 as a working fluid in the simulation, these interactions can be neglected and the temperature limit exceeded. Although the simulations cover only one-eighth of the entire domain, the results are presented for the entire 1 km^2 area. Assuming an injection over-pressure of 10 bar and a production under-pressure of 10 bar relative to the reservoir pressure, results are obtained for each of the cases. Computations are performed using water as a working fluid only at one pressure of 100 bar since the pressure has little effect on the thermodynamic properties of water. However, the reservoir pressure with CO_2 as a working fluid was varied at 45 bar, 100 bar, 200 bar, and 500 bar. The initial reservoir temperature is 200°C with an injection temperature of 20°C. Various parameters used in simulations are given in Table 4.1, additional needed parameters have been based obtained from the reference paper [21].

Table 4.1: Reservoir properties used in the base case simulations

Reservoir Thickness	305 m
Fracture spacing	50 m
Permeable volume fraction	2%
Permeability	$50.0*10^{-15}$ m^2
Porosity in the permeable domain	50%
Rock grain density	2650 kg/m^3
Rock specific heat	1000 J/kg-°C
Rock thermal conductivity	2.1W/m-°C

In previous research, often an external wellbore flow generator has been used; and then the wellbore flow option is specified in the GENER block of the TOUGH2 input file. However, in this study a TOUGH2-ECO2N code in conjunction with the GA-TOUGH2 code modified for CPI is

employed to replicate the correct wellbore flow. As discussed earlier, GA-TOUGH2 modified for CPI employs a solution searching technique to determine a time-dependent injection curve that approximates the desired injection cell pressure. The code relies on post-processing of the TOUGH2 output files to evaluate and then appropriately adjust the injection curve. In these simulations, the production cell is considered at a steady state condition of 10 bar less than the reservoir pressure. The injection cell is monitored using the GA-TOUGH2 CPI module with a specified threshold pressure of 10 bar greater than the reservoir pressure. An average pressure difference of 0.1 bar is established as the convergence criterion for the simulation. When GA-TOUGH2 obtains an injection curve with an average pressure difference less than 0.1 bar, the simulation is stopped and the injection profile is saved to be used as the equivalent wellbore flow injection. As in the case of CPI simulations reported in chapter 3, the fitness function for injection cell pressure in the present case monitoring is defined as:

$$\frac{\left|P_{threshold} - P_{injection}(Q_{CO_2})\right|}{Q_{CO_2}}$$

The parameters used in the simulations as input to the GA-TOUGH2 code are summarized in Table 4.2.

Table 4.2: Parameters used in the baseline simulation using GA-TOUGH2

Individuals per generation	6
Maximum number of generations	50
Natural selection removal	50%
Mutation rate	8%
Cross-over algorithm	Semi-Random Combination of Parents
Reservoir pressure with two different working fluids	45, 100, 200, 500 bar (CO_2) 100 bar (Water)
Threshold pressure	10 bar over the reservoir pressure

The results from the simulations of this study are compared with those of the previous study [21] can be seen in Figures 4.2 and 4.3. Mass flow rate for the entire well is determined by multiplying the simulation injection rate by 8 since only one-eighth of the domain is considered. Heat extraction rate G is determined by multiplying the full well mass flow rate by the enthalpy difference between the production and injection cell, it is given as:

$$G = Q_{CO_2}\left(h_{production} - h_{injection}\right)$$

where Q_{CO_2} denotes the mass flow rate of CO_2 and h the enthalpy at the given thermodynamic conditions. Present results and those of Pruess [21] are in good agreement as shown in Figures 4.2 and 4.3. Some differences in the two sets of results can be attributed to the difference in the injection profile generation in the two sets of simulations. In the current study overpressure in the injection cell is found due to a variable mass flow injection and is not specified as a constant as in the case of Pruess's simulations [21]. Although in the CPI scenario GA-TOUGH2 can find a solution close to the constant pressure case specified in the wellbore simulation of Pruess [21], there are nevertheless differences (approximately 0.1 bar) in the injection cell pressure between the two cases.

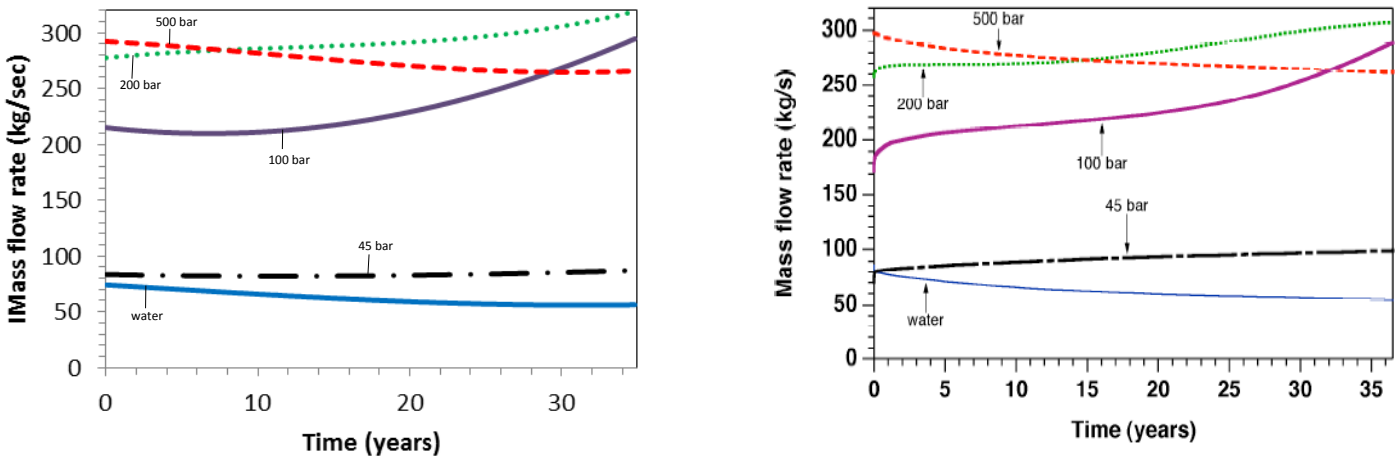

Figure 4.2: Comparison of mass flow rate for various reservoir pressures GA-TOUGH2 (left), Pruess simulations (right) [21]

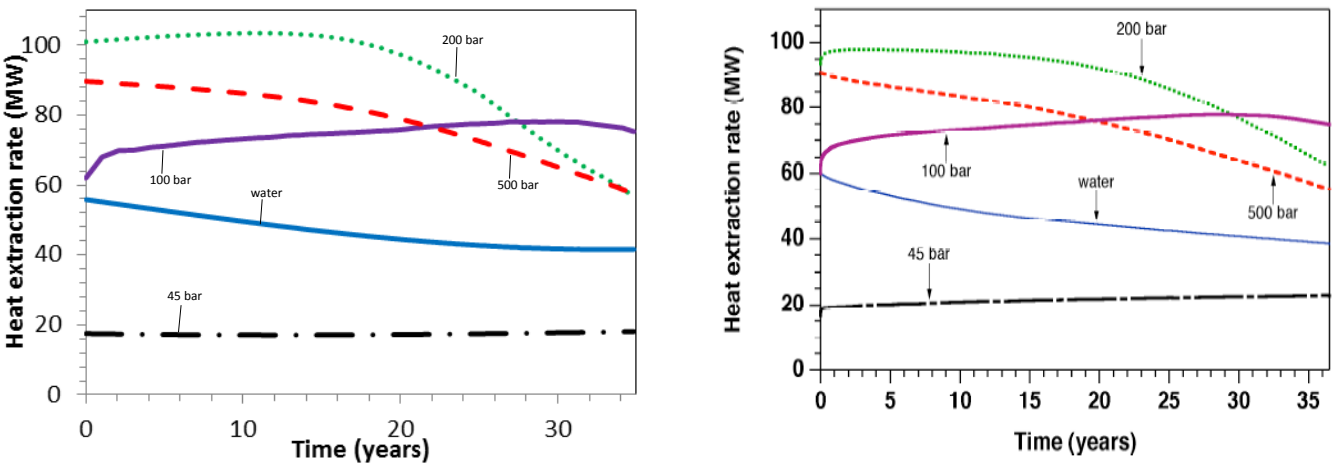

Figure 4.3: Comparison of heat extraction rate for various reservoir pressures GA-TOUGH2 (left), Pruess simulations (right) [21]

It is possible that with the use of a large number of generations in the GA-TOUGH2, the exact curves as found by Pruess [21] may be generated. However for the purpose of this study the results obtained to 0.1 bar accuracy are deemed acceptable. The benefit of using GA-TOUGH2 for modeling the cases studied by Pruess [21] is that it offers a general approach with its ability to adjust the injection rate as a result of the reservoir pressure. This is how an actual EGS is operated; a mass flow is initially specified, then the corresponding injection pressure is obtained based on which the mass flow is modified to adjust the pressure. In using an external wellbore simulator, there is little room to adjust the unknowns in the system, and the simulation is less able to adapt to changes in the injection parameters.

Overall the results obtained in this section are in close agreement with those of previous work; they give confidence to move forward with optimization studies which are reported in the next section. Although these simple simulations were replications of previous results, they are an important first step for optimizations of EGS. Using the same approach it is possible to define the fitness function slightly differently and optimize the variable injection rate using different variables. Using this methodology, one can monitor the water concentration in the production flow, monitor the

temperature profile and cold front migration as the reservoir ages, or monitor the heat extraction rate as a function of the injected CO_2 to determine the economics and efficiency of the system.

4.2 A case study of EGS optimization

In this section, the optimization of EGS for the management of the temperature profile with CO_2 as a working fluid is considered. The injection of CO_2 in a reservoir at 200 bar and 200°C is used for optimization. These reservoir conditions provide the greatest potential for maximum heat extraction from the reservoir of the cases presented previously. A superposition of a line of constant pressure on the mobility diagram of CO_2 shown in Figure 4.4 can be used to explain why this injection scenario results in a higher heat extraction rate.

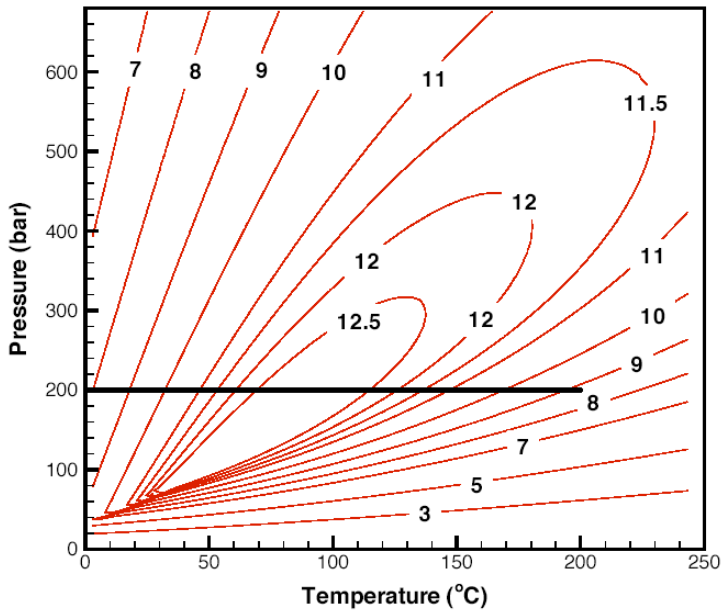

Figure 4.4: Variation in mobility of CO_2 with pressure and temperature (line of constant pressure shown in black at 200 bar) [13]

Following the line of constant pressure from the production temperature to the injection temperature, it can be noted that the mobility of CO_2 changes as the reservoir temperature changes at constant pressure. As the temperature in the reservoir cools below 200°C, the mobility of CO_2 increases from approximately $8*10^6$ s/m^2 to over $12.5*10^6$ s/m^2 at a temperature near 100°C. Hence as the reservoir cools, more CO_2 is able to move through the system and thus counteracts some of the effects of the cooling on heat extraction rate. Figure 4.5 shows the temperature of the production stream over the life span of the geothermal system.

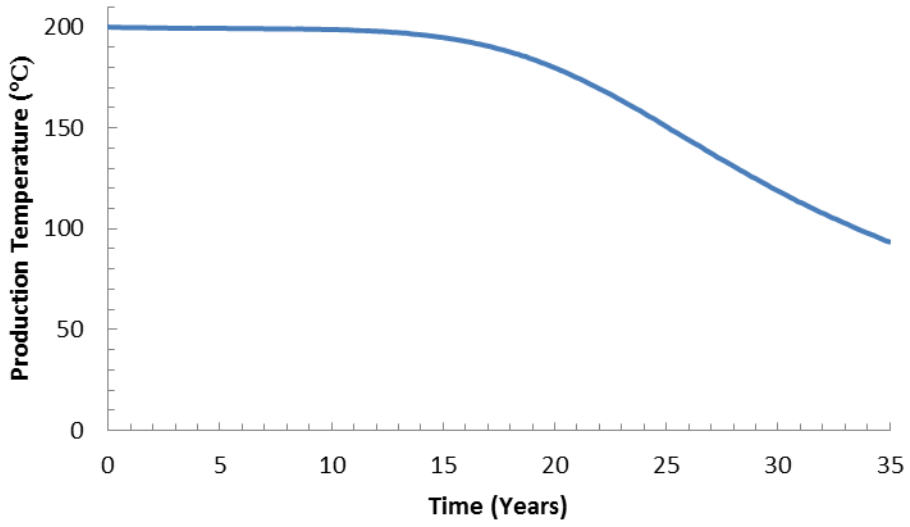

Figure 4.5: Temperature profile of the production stream for baseline case

For the first 15 years of operation of the system, the temperature of the production remains nearly constant with minimal temperature drop in the production stream; consequently there is a relatively constant heat extraction rate during the first 15 years of operation. After 15 years, the temperature begins to drop more rapidly and the heat extraction rate follows a similar decline. There is however a

lag to the heat extraction rate drop-off due to the increase in mobility with a decrease in temperature as discussed previously. The higher mobility allows for a higher flow rate in the system and thus helps in delaying the effects of the migrating cold front. The higher flow rate creates a positive feedback relationship to the temperature decline since the higher flow rate results in greater heat extraction and results in larger reservoir cooling. This relationship between the flow rate and temperature continues to decrease the temperature of the reservoir as heat is extracted from the system quicker than it can be replenished from the surrounding areas. Eventually, it becomes impossible to achieve an optimal heat extraction rate since the production temperature becomes too low. At this point the well has reached its life expectancy and cannot efficiently generate power.

4.3 Temperature Profile Optimization with a Constant Mass Injection

It is widely accepted that the minimum temperature for generating power from a geothermal reservoir is 100°C [22]. Below this temperature there is not enough energy in the fluid to generate power efficiently. It can therefore be assumed that in an EGS the reservoir temperature must be maintained above 100°C, otherwise the well will be at risk of shut-down. For the specific case of a reservoir with 200 bar pressure discussed in section 4.2, once the temperature begins to drop below ~100°C the mobility of CO_2 also drops and thus it becomes more difficult to move the fluid through the system. It is important to maintain the temperature above 100°C in order to extract as much heat from the reservoir as quickly as possible with a high mass flow rate. The selection of a temperature threshold at 100°C is fairly arbitrary and is chosen here simply since it is seen as the minimum temperature required to generate power. Although a wide range of temperatures over

100°C can be considered for optimization, in this study this threshold 100°C of is chosen as an example of proof-of-concept.

There is a balance between subjecting the reservoir to as high a flow rate as possible and to maintain the temperature of the production well above the desired temperature threshold. An ideal injection scenario should be able to establish the highest possible mass flow rate in the system which allows for a temperature above the specified threshold throughout the life of the well. Therefore the temperature profile of the production well is optimized such that the specified threshold temperature is reached at the time of well shut-down time. GA-TOUGH2 code is used to optimize the temperature of the production well for a constant injection rate. Later, using the information from this simulation, a constant pressure study is conducted.

The temperature of the production well for the baseline case with reservoir pressure of 200 bar and temperature of 200°C at well shut down time of 35 years is taken to be 93°C. If heat extraction ceases when the production temperature drops below the threshold of 100°C, the well shut-down would occur at 33.5 years. This would essentially halt the generation of power and may result in poor economics for the power generating utility. In this study, an optimization is conducted to extend the production life of this well by optimizing the temperature profile of the production stream. The injection rate range is established by brute force simulations at constant mass injections of 20kg/sec, 30 kg/sec, and 40kg/sec. It was found that the respective production temperatures at 35 years are 181.8°C, 124.1°C, and 82.0°C. Therefore it can be concluded from the brute force simulations that the optimal constant mass injection rate will be between 30 and 40 kg/sec.

The fitness function for this optimization is defined as follows:

$$F = \frac{1}{|End\ Time\ Production\ Temperature - Threshold\ Temperature| + 1}$$

where threshold temperature is considered as 100°C, and the end time production temperature is read from the FOFT file produced from TOUGH2 at the end of the simulation (at 35 years). The absolute value allows for end time production temperatures greater or less than the threshold temperature. The addition of 1 in the denominator prevents division by zero if the end time production temperature equals the threshold temperature. It can be seen that the optimal injection rate will have a fitness equal to or close to 1. Convergence is achieved when F reaches a value very close to 1. The parameters used in GA-TOUGH2 for this optimization are given in Table 4.3

Table 4.3: Parameters used in GA optimization of temperature profile with constant mass injection

Individuals per Generation	6
Maximum Number of Generations	50
Natural Selection Algorithm	50%
Mutation Rate	8%
Cross-Over Algorithm	Semi-Random Combination of Parents
Injection Range (for 1/8 of computational domain)	30-40 kg/sec

The GA convergence history for this case is shown in Figure 4.6; the optimal injection rate is 34.92 kg/sec for the model domain considered, or 279.36 kg/sec (34.92 kg/sec *8) for the entire reservoir.

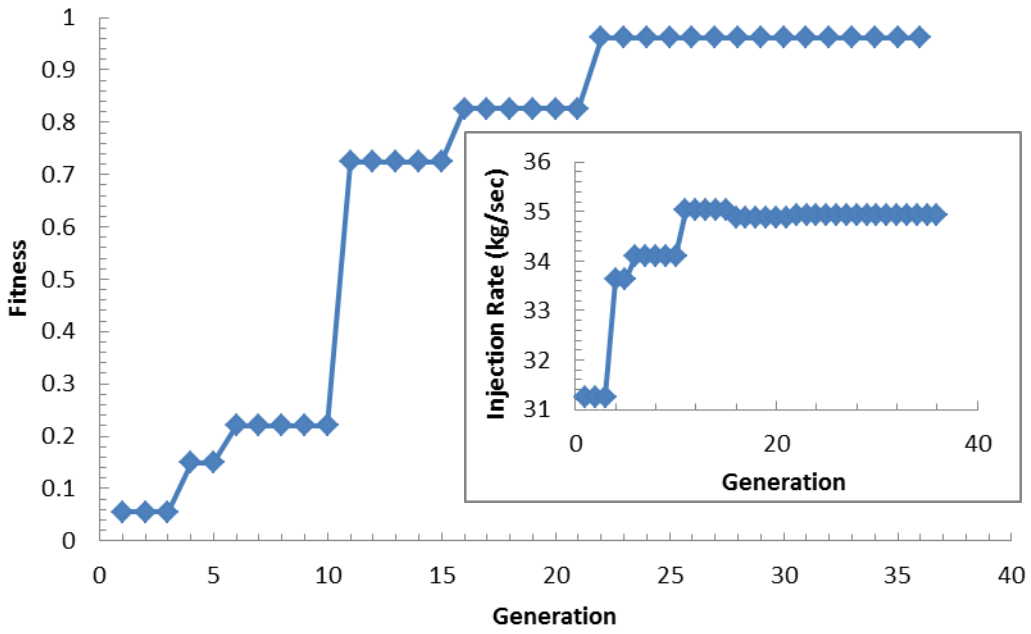

Figure 4.6: GA convergence history for temperature profile optimization with constant mass injection rate

The injection rate of 34.92 kg/sec gives a production temperature of approximately 100.04 °C at 35 years. This is a significant improvement in the temperature profile from the original case, as the constant mass injection is now able to maintain the desired production temperature for the entire lifespan of the well. The resulting temperature profile for this case is shown in Figure 4.7. An enlarged view of the last 15 years of well life (shown on the right of Figure 4.7) shows the true effect of the temperature optimization; the GA result shows a slower decline in temperature and does not reach the threshold value until the end of the well life.

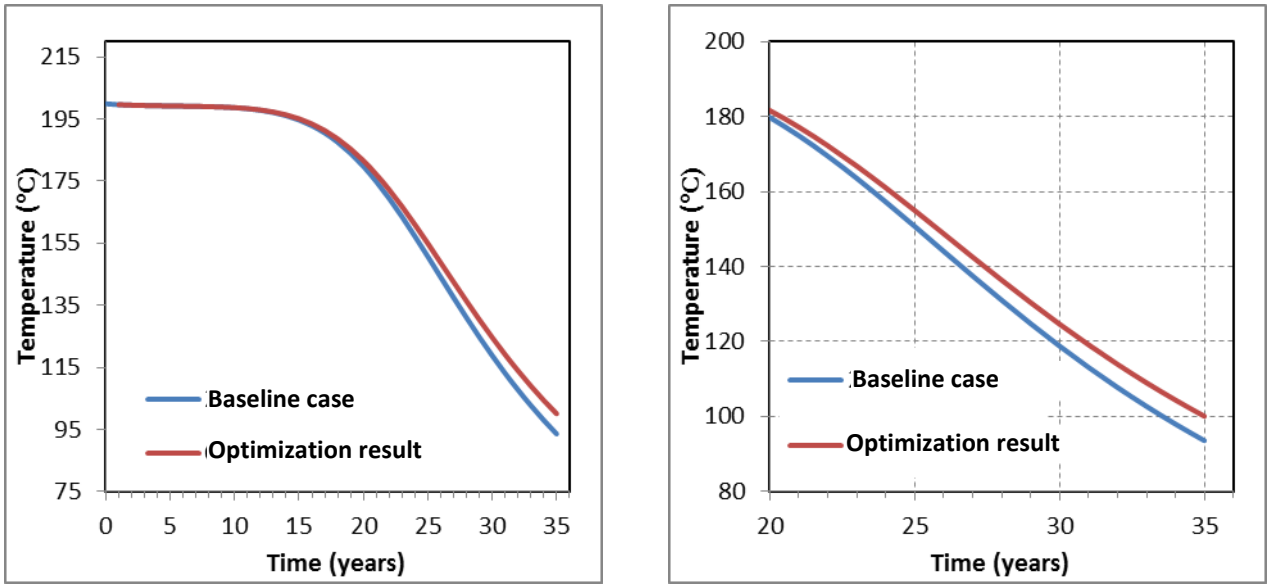

Figure 4.7: Comparison of baseline (blue) and optimized (red) production well temperature profiles for entire life (left) and final 15 years of life (right)

Although the results for a constant mass flow rate show promise for production temperature control, they are not an accurate indicator of how a real injection scenario would be executed. In addition, the constant mass flow rate does not account for the large changes in mobility of the fluid with time and thus does not produce the optimal heat extraction rate. The results for the constant mass flow rate are based on an average value for the entire life of the system and does not include any variability in mass flow rate. Figure 4.8 shows a comparison of injection cell pressure as a function of time for the baseline case and the optimized case with constant mass flow rate injection.

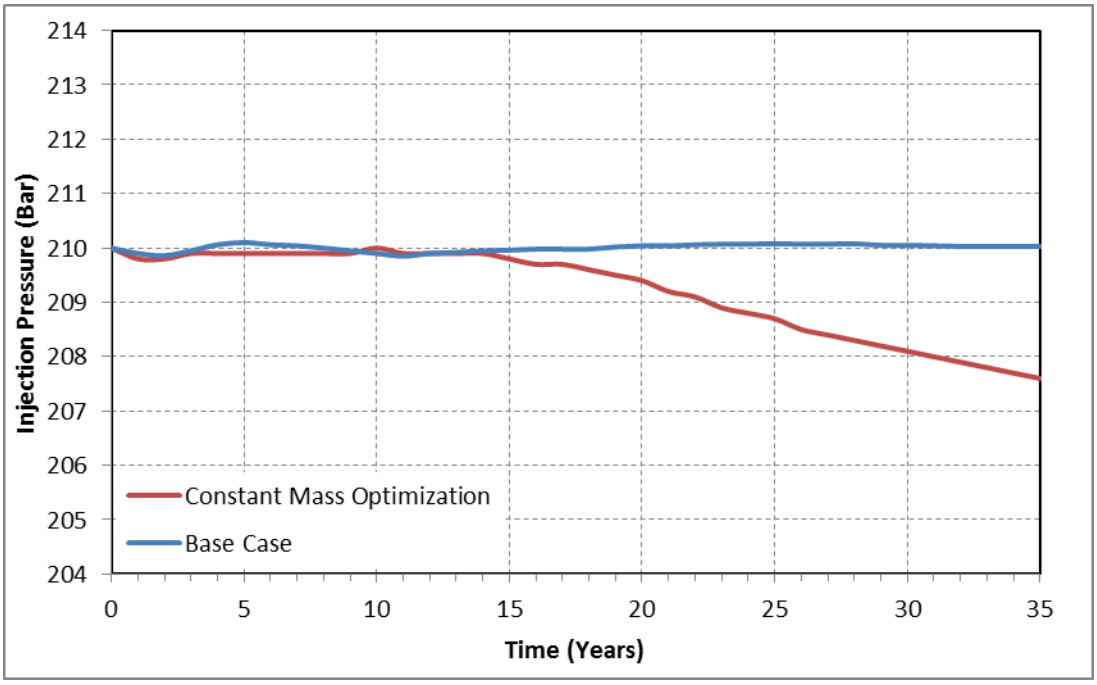

Figure 4.8: Comparison of injection pressure between the baseline case (blue) and optimized case (red) for constant mass injection rate

From Figure 4.8, it can be noticed that the injection cell pressure for the constant mass optimization decreases with time. As the reservoir cools, the mobility of the CO_2 increases and thus flows through the system more easily. There is a smaller restriction on the flow of CO_2 and therefore the pressure of the injection cell decreases with time. This is not an advantageous approach since it does not allow for the maximum heat extraction rate. An ideal injection scenario would be at a constant pressure injection while keeping the desired temperature profile for the life of the well.

4.4 Temperature Profile Optimization Using a Constant Pressure Injection

While the previous optimization in section 4.3 for a constant mass injection rate gave promising results, it is not an accurate representation of how fluid would be injected in a real EGS. As discussed in the first section 4.1, the mobility of CO_2 changes significantly with change in temperature. For the reservoir pressure of 200 bar considered in this study the CO_2 will be able to move more easily at lower temperatures which will correspond to a higher mass flow rate for a constant pressure injection. In order to optimize the temperature profile for constant pressure injection GA-TOUGH2 is run at different pressures than the original base case. The injection overpressure is determined by taking the average injection pressure from GA-TOUGH2 optimization already for constant mass injection for the first 15 years. This new injection pressure is specified as the threshold pressure for the CPI study. The GA parameters are the same as those for the baseline case simulations with the exception of a different threshold pressure, they are shown in Table 4.4.

Table 4.4: Parameters for constant pressure injection GA optimization

Individuals per Generation	6
Maximum Number of Generations	500
Natural Selection Algorithm	50%
Mutation Rate	10%
Cross-Over Algorithm	Semi-Random Combination of Parents
Threshold Pressure	209.3 bar

The GA convergence history for the fitness function based on pressure difference is shown in Figure 4.9, the inset figure shows the best time-dependent injection profile for a CPI scenario.

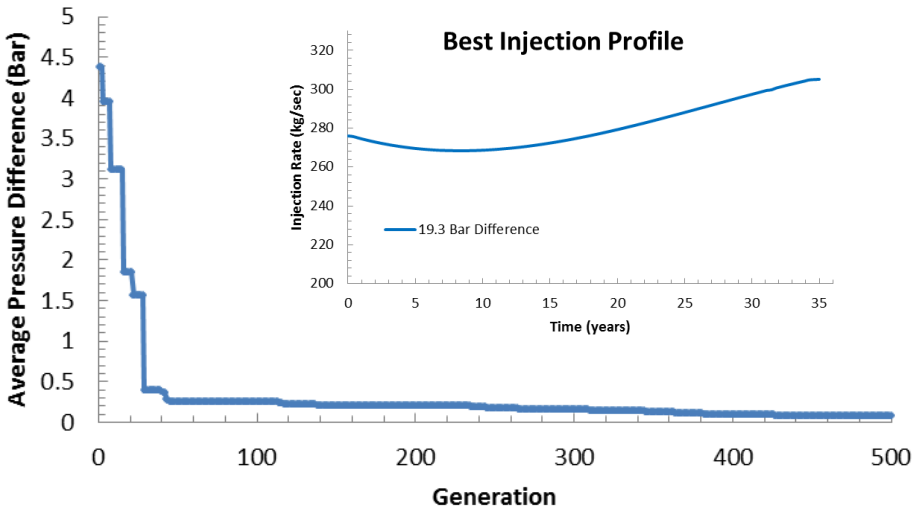

Figure 4.9: GA convergence history for temperature profile optimization with constant pressure injection

The injection profile continues to evolve during the simulation; at approximately generation #400 the GA determines an injection profile with an average pressure difference of 0.08 bar and this remains the optimal injection profile for generations after #400. This average pressure difference is within the convergence criterion of 0.1 bar and satisfies the goal of finding an appropriate time-dependent injection rate for an injection cell pressure of 209.3 bar. As shown in the inset graph of Figure 4.9, the injection profile begins at a higher injection rate but as the pressure in the system is established it begins to decrease as the flow develops and finally rises to accommodate for the effects of reservoir cooling.

Figure 4.10 shows the production temperature profiles for the baseline case and the optimized constant pressure injection. For approximately the first 15 years of injection, the two profiles match very closely, however as time progresses the effects of the optimization can be noticed. The lower pressure case (19.3 bar difference) has a slower decline in temperature and is able to maintain the production temperature above 100 °C for the 35 years of the simulation. The corresponding heat extraction rates for the baseline case and optimized case are shown in Figure 4.11. Initially the heat extraction for the optimized case is less than that for the baseline case due to a lower mass flow rate. As the temperature for the baseline case reservoir begins to decline, its heat extraction rate also declines. After 25 years of injection, the optimized case has a greater heat extraction rate than the baseline case.

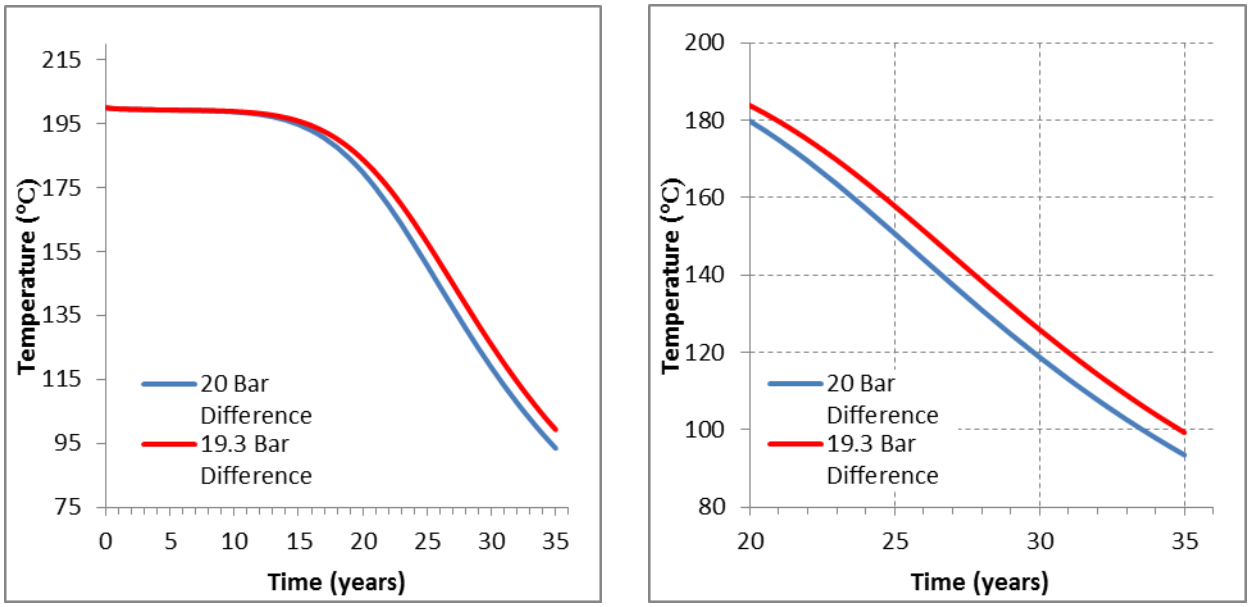

Figure 4.10: Comparison of temperature profiles between the baseline case (blue) and optimized case (red) for constant pressure injection

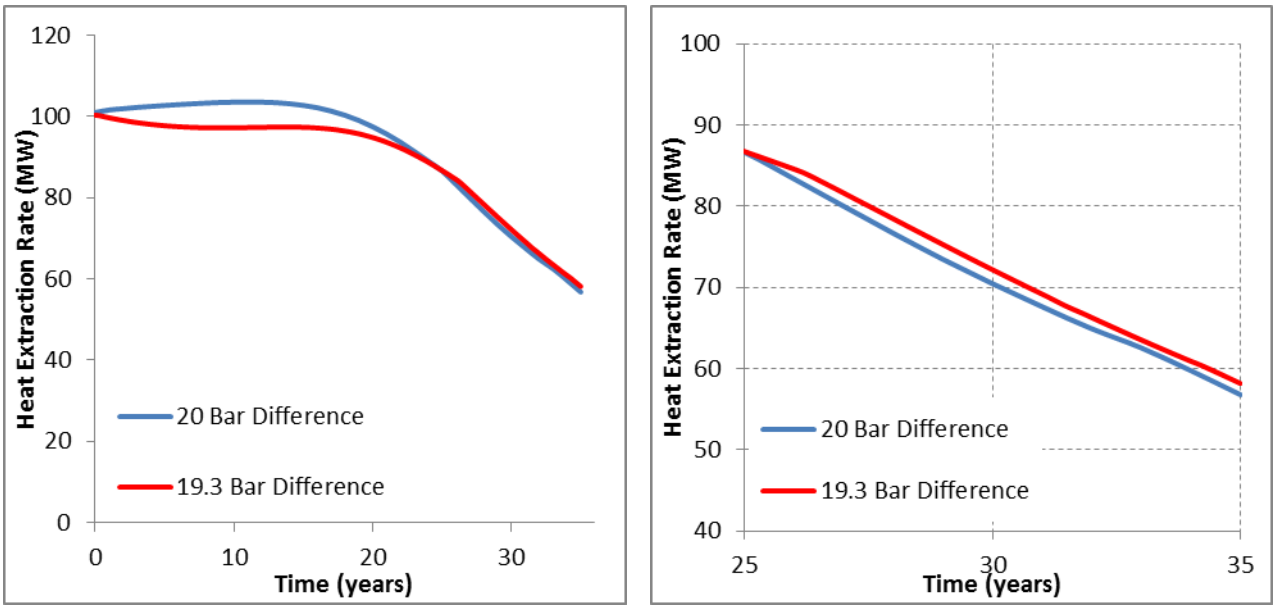

Figure 4.11: Comparison of heat extraction rates between the baseline case (blue) and optimized case (red) for constant pressure injection

While the cumulative heat extraction rate of the optimized case is less than that of the baseline case, management of the temperature profile results in a more sustainable heat extraction rate. This result may be helpful for future studies on optimization of the heat extraction rate instead of the temperature profile. The heat extraction rate optimization would be able to accommodate for the reservoir cooling effects on both enthalpy and mobility of CO_2.

The results presented in this section demonstrate the ability of GA-TOUGH2 to efficiently manage the temperature profile of an EGS. It is shown that for an arbitrarily specified temperature threshold in the production well, the GA-TOUGH2 is able to optimize a constant mass and a constant pressure injection scheme. This offers a promising approach for the development of a sustainable EGS and may help in the EGS technology a step closer to commercialization.

Chapter 5

Conclusions and Future Research

5.1 Conclusions

In this thesis numerical simulations and optimizations of two problems in Carbon Utilization and Storage have been conducted. The first simulation dealt with a problem relevant to enhanced gas recovery (EGR) using CO_2. The second simulation dealt with a problem relevant to an enhanced geothermal system (EGS) using supercritical CO_2. In both the studies, a high pressure CO_2 fluid was injected in the reservoir/formation and its migration was simulated using the TOUGH2 numerical solver. Code validations studies for both EGR and EGS were first conducted using TOUGH2 with modules EOS7C and ECO2N respectively. A close agreement was obtained between previous studies reported in the literature and the present study. After the validation, optimization studies were conducted on these baseline cases using the genetic algorithm based optimizer GA-TOUGH2. The original GA-TOUGH2 program was modified to accommodate the specific TOUGH2 modules (EOS7C and ECO2N) and for different fitness/objective functions. Simulations first considered time-independent injections to optimize the recovery factor for EGR and the temperature profile in EGS. Optimized simulations resulted in a recovery factor approximately 5% greater than the non-optimized case for EGR they also resulted in a shorter methane extraction time. For the EGS case, an optimal injection rate was determined to achieve the temperature threshold at the predetermined end-time for the production well thus allowing heat extraction to occur for the entire well life. Following up on the time independent simulations, similar optimization studies were carried out using time dependent injection rates. The time-dependent optimizations

utilized a Bezier curve to find an optimal injection rate profile to maintain a constant injection pressure in the injection well. The EGR constant pressure injection optimization resulted in greater methane production rate compared to the baseline case, a shorter overall extraction time, and a safe management of the injection cell pressure below an allowable threshold value. For EGS the time-dependent constant pressure injection optimization resulted in a better management of the temperature profile of the production stream, a maintaining of the injection pressure below the threshold, and a heat extraction for the entire well life. The results obtained from these optimization studies demonstrate how improvements can be made to various injection scenarios to determine the optimal injection of CO_2. The efficient use of captured CO_2 is important for the success of CCUS projects. It is shown that the optimization of CCUS projects can make them more economically feasible.

5.2 Future Research

There are several aspects of optimization where future research in this area could be directed. Further studies in enhanced gas recovery (EGR) may focus on non-isothermal effects of the CO_2 interactions with CH_4 and their effects on reservoir simulations. Additionally, simulations utilizing different reservoir conditions may yield different gas extraction rates since the density and viscosity of supercritical CO_2 vary greatly with changes in temperature and pressure. Future work in enhanced geothermal systems (EGS) should focus on the 3-D simulations of the reservoir and its effects on the density of CO_2 and the optimization. It is anticipated that inclusion of the density effects of CO_2 would yield significantly different results than those found in this study. In order to provide a more accurate depiction of real-world EGS, the density effects of CO_2 must be included. Further optimization studies should consider the initial reservoir development stage by finding an optimal

injection rate to minimize the time of reservoir development. Additionally, simulations should be performed to find an optimal constant heat extraction rate which is more desirable than the determination of an optimal temperature profile. The optimization study in this thesis shows a declining heat extraction rate due to reservoir cooling; it may be possible to find a lower injection rate that includes the effects of reservoir cooling and the resulting changes to CO_2 mobility to find an optimal constant heat extraction rate.

In both EGR and EGS, the advancement and large scale commercialization of the technology will depend on both computer simulations and laboratory and field experiments. For the further advancement of these processes it is be important to begin pilot plant and experimental studies along with the computer simulations. Computer simulations require data from pilot plant studies for validation but once validated can provide useful information for large industrial scale development of EGR and EGS projects.

References

[1] International Energy Outlook 2010, US Energy Information Administration, Office of Integrated Analysis and Forecasting, US Department of Energy, July 2010.

[2] Dr. Pieter Tans, NOAA/ESRL (www.esrl.noaa.gov/gmd/ccgg/trends/) and Dr. Ralph Keeling, Scripps Institution of Oceanography (scrippsco2.ucsd.edu/).

[3] Global, Regional, and National Fossil-Fuel CO2 Emissions. Carbon Dioxide Information Analysis Center Oak Ridge national Laboratory

[4] B. Metz, O. Davidson, H. de Coninck, M. Loos, and L. Meyer (eds.), IPCC Special Report on Carbon Dioxide Capture and Storage, *Cambridge University Press*, 2005.

[5] Workshop on Numerical Models for Carbon Dioxide Storage in Geological Formations, *University of Stuttgart* website, http://www.iws.uni-stuttgart.de/CO2-workshop/

[6] Overview of Carbon Storage Research, US Department of Energy, Office of Fossil Energy, 2014.

[7] van der Burgt, M.J., J. Cantle, V.K. Boutkan, "Carbon dioxide disposal from coal-based IGCC's in depleted gas fields," Energy Convers. Mgmt., 33(5–8) (1992), 603.

[8] Blok, K., R.H. Williams, R.E. Katofsky, C.A. Hendricks, "Hydrogen production from natural gas, sequestration of recovered CO2 in depleted gas wells and enhanced gas recovery" Energy, 22 (2/3) (1997), 161.

[9] Brown, D., 2000. "A hot dry rock geothermal energy concept utilizing supercritical CO2 instead of water." *Proceedings of the Twenty-Fifth Workshop on Geothermal Reservoir Engineering, Stanford University*, pp. 233-238.

[10] Fouillac, C., B. Sanjuan, S. Gentier, and I. Czernichowski-Lauriol, 2004. "Could sequestration of CO_2 be combined with the development of enhanced geothermal systems" *Third Annual Conference on Carbon Capture and Sequestration, Alexandria, VA.*

[11] Carbon Capture and Sequestration Project Database. Carbon Capture and Sequestration Technologies at Massachusetts Institute of Technology. Updated 2013.

[12] Phase Diagram, General properties and uses of carbon dioxide. Global CCS Institute. 2014

[13] Pruess K. Enhanced geothermal systems (EGS) using CO2 as working fluid - a novel approach for generating renewable energy with simultaneous sequestration of carbon, *Geothermics,* Vol. 35, pp. 351-367, 2006.

[14] K. Pruess, TOUGH2: A General Numerical Simulator for Multiphase Fluid and Heat Flow, *Lawrence Berkeley Laboratory Report LBL-29400*, Berkeley, CA, 1999.

[15] K. Pruess, C. Oldenburg, and G. Moridis, TOUGH2 User's Guide, Version 2.0 (revised), *Lawrence Berkeley Laboratory Report LBL-43134*, Berkeley, CA, 2011.

[16] Zhang, Zheming, "Numerical Simulation and Optimization of CO2 Sequestration in Saline Aquifers" (2013). *Electronic Theses and Dissertations.* Paper 1097.

[17] PetraSim User Manual, *Thunderhead Engineering* website, http://www.thunderheadeng.com/downloads/petrasim/PetraSim-4-manual.pdf

[18] A. Ebigbo, J. M. Nordbotten, and H. Class, Numerical Investigations of CO2 Sequestration in Geological Formations: Problem-Oriented Benchmarks, Problem 2, Enhanced CH4 Recovery in Combination with CO2 Storage in Depleted Gas Reservoirs, *R&D-Program of GEOTECHNOLOGIEN* website, http://www.hydrosys.uni-stuttgart.de/co2-workshop/Problem2.pdf

[19] C.M. Oldenburg, K. Pruess, and S.M. Benson, Process Modeling of CO_2 Injection into Natural Gas Reservoirs for Carbon Sequestration and Enhanced Gas Recovery. Earth Sciences Division, lawrence Berkeley National Laboratory, Berkeley, California 94720. January 15, 2001.

[20] Bézier curve, *Wikipedia* website, http://en.wikipedia.org/wiki/B%C3%A9zier_curve

[21] Pruess, K. (2008), "On production behavior of enhanced geothermal systems with CO2 as working fluid," *Energy Conversion and Management*, **49**, 1446–1454

[22] Geothermal Electricity Production. Learning about Renewable Energy, National Renewable Energy Laboratory. U.S. Department of Energy http://www.nrel.gov/learning/re_geo_elec_production.html

Vita

James H. Biagi

Degrees

M.S. Department of Mechanical Engineering & Materials Science, Washington University in St Louis, May 2014

B.S. Department of Mechanical Engineering & Materials Science, Washington University in St Louis, May 2014

Publications

James Biagi, Ramesh Agarwal, Optimization of Enhanced Gas Recovery (EGR) using a Genetic Algorithm *13th Annual Conference on Carbon Capture Utilization and Storage*, Pittsburg, PA, May 2014.

James Biagi, Ramesh Agarwal, Optimization of Enhanced Geothermal Systems (EGS) with Constant Pressure Injection of CO_2 *13th Annual Conference on Carbon Capture Utilization and Storage*, Pittsburg, PA, May 2014.

James is currently working as a project engineer for Alberici Enterprises in the Energy Sector.

May 2014